MISCELLANEOUS PAPER N-73-2

FUNDAMENTAL EXPERIMENTS IN GROUND SHOCK PHENOMENOLOGY

by

J. G. Wallace, J. Fowler

March 1973

Sponsored by Office, Chief of Engineers, U. S. Army

Conducted by U. S. Army Engineer Waterways Experiment Station
Weapons Effects Laboratory
Vicksburg, Mississippi

MISCELLANEOUS PAPER N-73-2

FUNDAMENTAL EXPERIMENTS IN GROUND SHOCK PHENOMENOLOGY

by

J. G. Wallace, J. Fowler

March 1973

Sponsored by Office, Chief of Engineers, U. S. Army

Conducted by U. S. Army Engineer Waterways Experiment Station
Weapons Effects Laboratory
Vicksburg, Mississippi

ARMY-MRC VICKSBURG, MISS.

THE CONTENTS OF THIS REPORT ARE NOT TO BE USED FOR ADVERTISING, PUBLICATION, OR PROMOTIONAL PURPOSES. CITATION OF TRADE NAMES DOES NOT CONSTITUTE AN OFFICIAL ENDORSEMENT OR APPROVAL OF THE USE OF SUCH COMMERCIAL PRODUCTS.

ABSTRACT

This paper describes a technique which can be used to create a well defined directly-induced seismic energy source exclusive of any airblast effects. It was shown that spherical masses impacting on the ground surface produced ground motions which could be correlated with motions produced by high explosion tests.

The tests conducted during this study included twenty-six spheres of varying size and density with weights ranging from 9 lb to 2,275 lb. Geophones were placed at various distances from the impact epicenter to measure ground surface particle velocity. An accelerometer was mounted on the sphere to monitor the deceleration during impact on the ground surface. Empirical equations were developed for the peak vertical particle velocity, period, wave group velocity and impact crater dimensions in terms of energy level and distance from the epicenter of the source. The impact data obtained at WES was correlated with high explosive data obtained during the MIXED COMPANY test conducted in Colorado.

FOREWORD

This investigation was sponsored by the Office, Chief of Engineers, Department of the Army, under appropriation No. 2122040 2081306 p501A, Project No. 4A0621101A91D, In-House Laboratory Independent Research Program. These experiments were conducted in connection with ground motion studies of wave propagation resulting from dropping spherical weights on the ground surface. The field investigations were performed from 22--26 May 1972.

The work was accomplished under the general supervision of Mr. G. L. Arbuthnot, Jr., Chief of the Weapons Effects Laboratory, and under the direct supervision of Mr. L. F. Ingram, Chief of the Physical Sciences Branch. Engineers of the Waterways Experiment Station (WES) who were actively engaged in the field investigations, analysis, and report phases of this study were Messrs. J. G. Wallace, J. L. Drake, Jack Fowler and C. E. Joachim. The report was prepared by Messrs. J. G. Wallace and Jack Fowler.

COL Ernest D. Peixotto, CE was Director of WES during the conduct of the investigation and publication of this report. Mr. F. R. Brown was Technical Director.

CONTENTS

LIST OF FIGURES

ABBREVIATIONS AND SYMBOLS

W	Weight of sphere, lb
D	Diameter of sphere, ft
H	Height of drop of sphere, ft
a_p	Peak deceleration of sphere during impact, ft/sec^2
T_d	Duration of deceleration pulse, sec
v_o	Impact velocity of sphere, ft/sec
t	Time, sec
V_{r1}	Group velocity of first surface wave, ft/sec
V_{r2}	Group velocity of peak surface,wave, ft/sec
V_1	Peak to peak vertical particle velocity of first wave group, ft/sec
V_2	Peak to peak vertical particle velocity of peak wave group, ft/sec
T_1	Period of first wave group, sec
T_2	Period of peak wave group, sec
V_i	$(V_2/2$, peak vertical velocity for impact seismic sources, ft/sec
V_e	Peak vertical velocity for high explosive seismic sources, ft/sec
E	Total energy or yield, lb-TNT
$(C_r)_i$	Crater radius from impacting spheres, ft
$(C_d)_i$	Crater depth from impacting spheres, ft
$(C_{rt})_e$	True crater radius from high explosives, ft
$(C_{dt})_e$	True crater depth from high explosives, ft
g	Acceleration of gravity, 32.2 ft/sec
R	Range from seismic source, ft

γ Soil density, 116 lb/ft^3

σ_p Average vertical stress during impact of sphere, lb/ft^2

CONVERSION FACTORS, BRITISH TO METRIC UNITS OF MEASUREMENT

British units of measurement used in this report can be converted to metric units as follows.

Multiply	By	To Obtain
inches	2.54	centimeters
feet	0.3048	meters
cubic inches	16.3871	cubic centimeters
pounds	0.45359237	kilograms
pounds per square inch	0.070307	kilograms per square centimeter
pounds per cubic foot	16.0185	kilograms per cubic meter
inch-pounds	0.011521	meter-kilograms
inches per second	2.54	centimeters per second

FUNDAMENTAL EXPERIMENTS IN GROUND SHOCK PHENOMENOLOGY

PART I: INTRODUCTION

Background

1. Analyses of ground shock wave forms produced by explosions reveal the various modes of seismic energy propagation and dissipation with range from the source. Waveforms for cratering bursts are characterized by relatively simple high amplitude and high frequency compression and shear waves in the region near the explosion but at greater ranges the surface motion is characterized by large amplitude and low frequency Rayleigh waves. There is currently much interest in developing prediction techniques for the "ground roll" type motions in the far-out regions resulting from large nuclear explosions.

2. In spite of the numerous explosion effects studies conducted to date and the state of seismic wave detection, the basic phenomenology of seismic wave propagation in the far-out region is not clear. In general, the military community has been concerned with ground shock closer to the source while the researchers concerned with the relatively weak seismic motions were primarily interested in long range detection, earthquakes, and arrival times.

3. The phenomena is complicated by influences of geometry, boundary conditions (air-ground interface and geologic layering), partitioning and coupling of airblast and cratering induced energy, and yield or effective energy of the source.

Objectives

4. The objectives of this investigation were (a) to provide an energy source exclusive of airblast effects which would isolate the effects of cratering induced energy, (b) to measure the surface motions at various ranges from the source and (c) to demonstrate the development of Rayleigh waves and the influence of source energy on wave characteristics such as amplitude and frequency as a function of range and crater geometry.

5. Fundamental ground shock experiments were conducted using free-falling spherical weight impacts as a seismic source. The results of these experiments will be used to develop prediction equations for the surface motion as a function of effective energy input, impulse, range, and crater dimensions.

PART II: SIMILITUDE REQUIREMENTS

Introduction

6. A dimensional analysis of a phenomenon can provide only qualitative rather than quanitative relationships, but when it is combined with a set of carefully designed experiments it can provide quanitative and accurate prediction equations.

7. The initial step in any investigation utilizing dimensional analysis is the determination of the variables which influence the phenomenon. It is then possible to express each variable in terms of some basic dimensions such as force, length and time. The Buckingham Pi Theorem states that: "The number of variables required to describe a phenomena is the difference between the original number of variables, N, and the number of basic dimensions, s, involved." In this case the system of basic dimensions used are force F, length L, and time T.

8. The significant variables assumed to be associated with ground surface motion for this study are tabulated below:

No.	Quanity	Basic Dimensions
1	W = weight of sphere	F
2	D = diameter of sphere	L
3	H = height of drop of spherical weight	L
4	a = deceleration of weight during impact	LT^{-2}
5	T_d = duration of acceleration pulse after impact	T
6	R = ground range	L
7	γ = soil density	FL^{-3}
8	V = peak to peak particle velocity at range, R	LT^{-3}
9	T = wave period	T
10	V_r = Rayleigh wave speed (group velocity)	LT^{-1}
11	g = acceleration of gravity	LT^{-2}
12	C_d = crater depth	L
13	C_r = crater radius	L

Since the site location will be the same for all tests, the parameters describing the soil are omitted.

9. A dimensional analysis of the phenomenon yields a general functional relationship of the following form:

$$F \left\{ \frac{WH}{R^4} , \frac{V^2}{gR} , \frac{V_r T}{R} , \frac{V}{V_r} , \frac{a}{g} , \frac{aT_d}{(gH)^{1/2}} , \frac{H}{C_d} , \frac{H}{C_r} , \frac{H}{R} , \frac{D}{R} \right\} = 0 \qquad (1)$$

Any other functional form of the relationship can be derived from this set of dimensionless products.

PART III: EXPERIMENTAL PROCEDURES

Spherical Weights

10. Spherically shaped weights of various weights, densities, and diameters were used during these experiments. All of the spheres were cast in existing molds at WES except for the 2275 lb cast iron demolition ball and the 11.38-lb aluminum ball. The density of the cement grout spheres was varied by changing the proportions of lead powder, ilmenite sand, iron powder, and styrofoam beads. A handling rod was cast into the heavy spheres to facilitate handling during the tests. Table 1 shows the diameter, weight, volume, density and material composition of the spheres used in the study. Figure 1 is a photograph of the cement grout spheres used in the tests.

Instrumentation

11. The instrumentation used for the ground surface motion measurements consisted of particle velocity transducers (PVT), and a particle acceleration transducer (PAT) which was mounted to selected spheres to measure the deceleration during impact (Figure 2). The PVT's and PAT were interfaced by compatible electronics to an analog FM magnetic recorder and an oscillograph recorder. Equipment and pertinent specifications are listed in Appendix A. A photograph of a PVT and the PAT is shown in Figure 3. An instrumentation block diagram is shown in Figure 4.

Table 1

Spherical Weights

Diameter ft	Weight lb	Volume ft	Density pcf	Material
1.34	266.00	1.260	211	Cement grout, lead powder, ilmenite sand, and iron powder
1.00	108.00	0.524	206	
0.81	58.00	0.278	208	
0.75	46.00	0.221	208	
0.59	21.00	0.108	195	
1.34	131.00	1.260	104	Cement grout, styroform beads
1.00	54.50	0.524	104	
0.81	28.50	0.278	102	
0.75	23.00	0.221	104	
0.59	10.00	0.108	93	
1.34	79.00	1.260	63	Cemented grout, styroform beads
1.00	33.00	0.524	63	
0.81	16.00	0.278	57	
0.75	13.00	0.221	59	
1.34	200.00	1.260	159	Cement grout, ilmenite sand
1.00	81.50	0.524	156	
0.81	44.00	0.278	158	
0.75	35.00	0.221	158	
0.59	16.00	0.108	149	
0.48	9.00	0.058	155	
2.13	2275.00	5.060	450	Cast iron
0.50	11.38	0.065	174	Aluminum
0.34	14.00	0.020	681	Bismuth
0.27	7.00	0.010	681	Bismuth

Figure 1. Cement Grout Spheres

Figure 2. Accelerometer Epoxied to 38 lb Bismuth Sphere

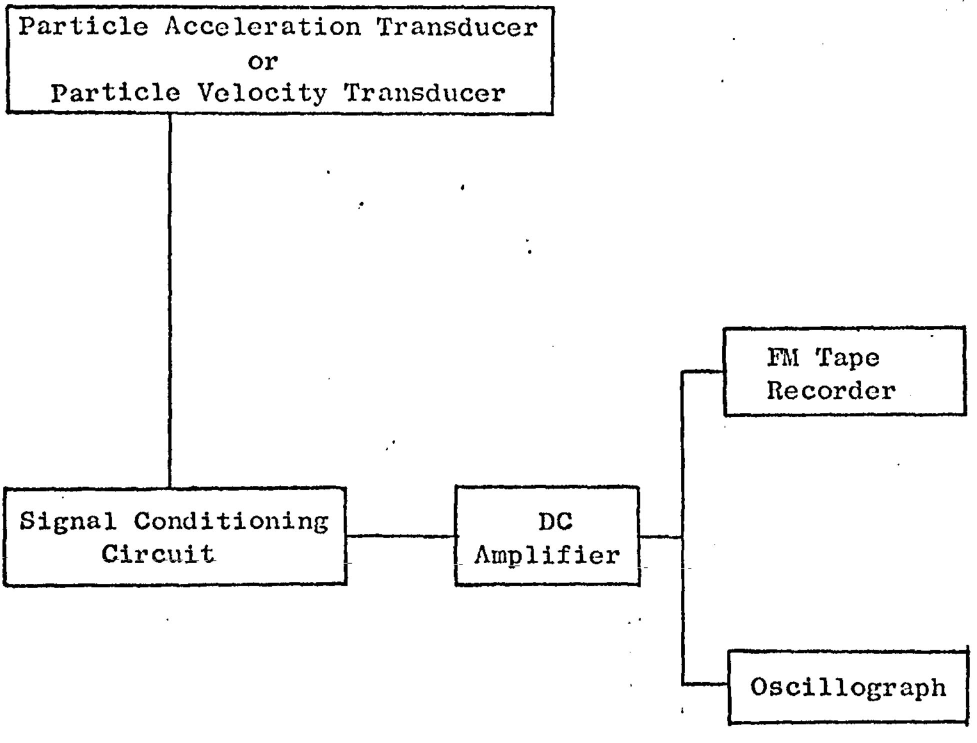

Figure 4. Instrumentation Block Diagram

Test Site Description

12. The test site was located east of the Weapons Effects Laboratory (Bldg. 5014) adjacent to the west side of "B" stream where previous geophysical tests (Reference 1) had been conducted. This site was designated WES Site No. 2 (Figure 5).

13. This site is located in a relatively flat creek bottom with the water table at approximately 12 ft. A 3- to 4-ft layer of silt (hydraulic fill) overlays the site, which originally consisted of loess. The geophysical tssts indicated that the near surface compression wave velocities varied from 1100-1500 ft/sec and the layer thickness varied from 11-13 ft. The velocities in the second layer varied from 4800-5300 ft/sec and the layer depth varied from 72-76 ft. The velocities in the third layer, which was limestone, ranged from 8900-9400 ft/sec. The limestone was recorded from a boring near the bridge crossing "B" stream on Ohio road to be at a depth of about 75 ft.

14. The previous vibratory tests conducted at this site indicated the shear wave velocity varied from 300-800 ft/sec from a depth of 5-75 ft, respectively.

Description of Tests

15. Prior to conducting the tests a 20 ft by 150 ft drop zone was prepared by grading off the turf with a bulldozer and finish graded with a motor patrol grader. A test site layout showing the drop zone and PVT locations is shown in Figure 6. Ten vertical sensing PVT's were buried flush with the ground surface and spaced on a line at

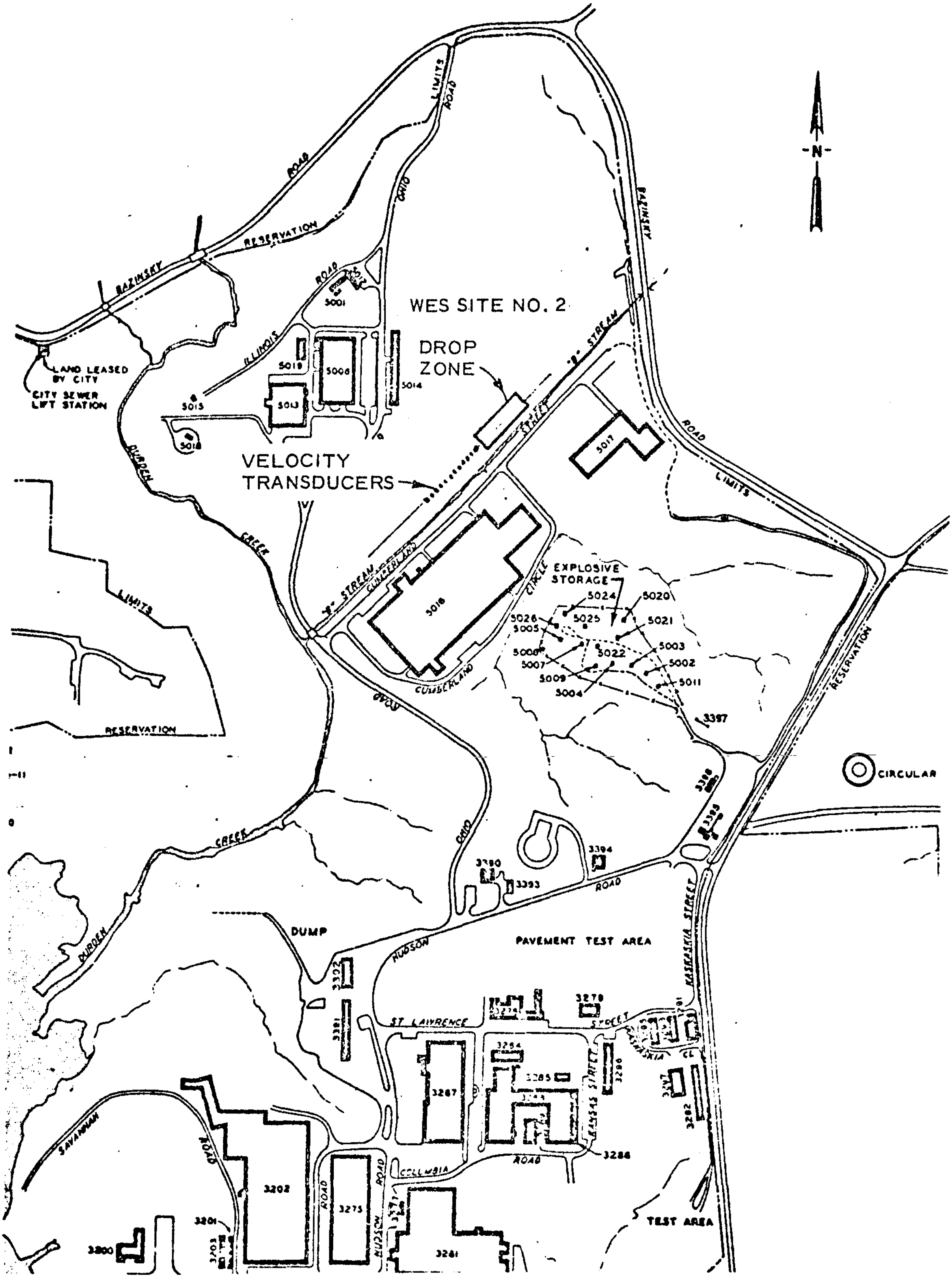

Figure 5. WES Site No. 2

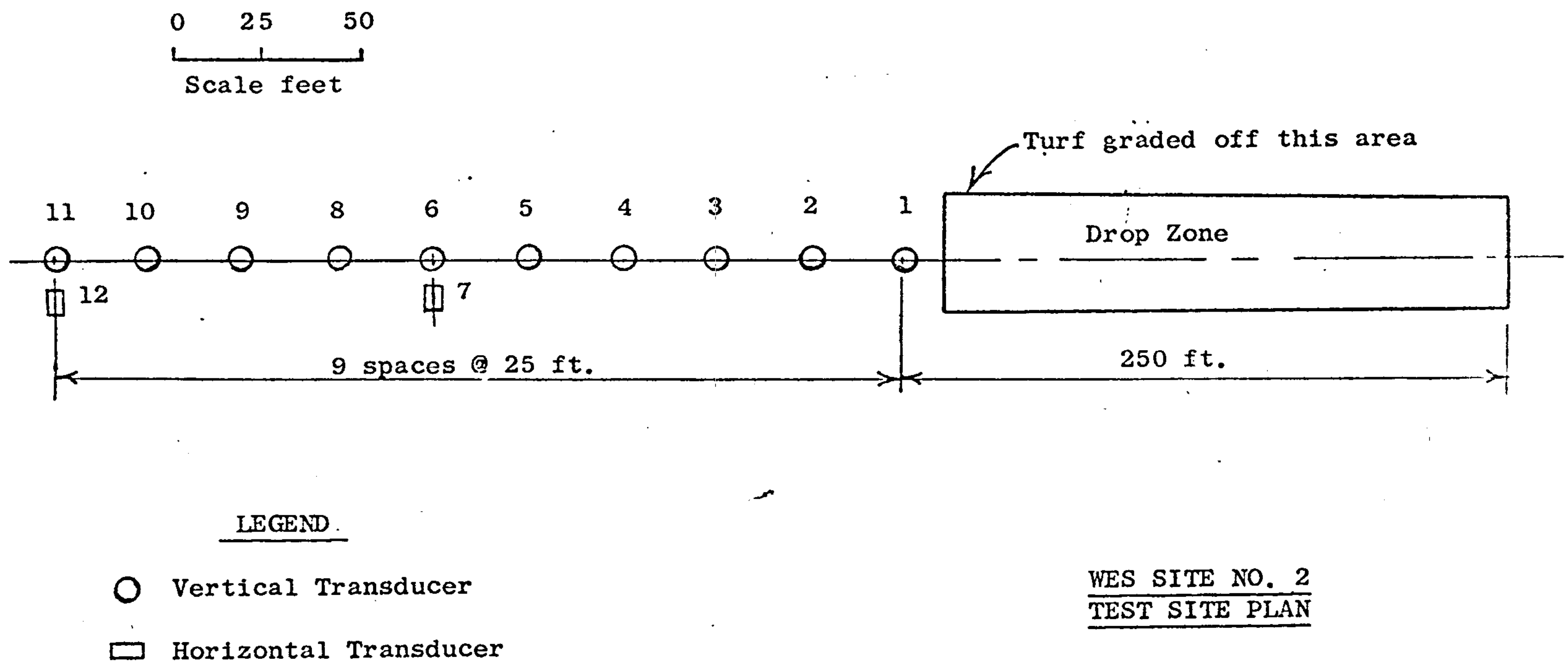

Figure 6. Test Site Plan View

25-ft intervals. Two horizontal sensing PVT's were buried and oriented in a radial direction to the drop zone and were located adjacent to vertical PVT's 6 and 12. Beginning with Test No. 71 an accelometer was mounted to the top of the spheres. To prevent the spheres from rotating as they fell, a line was passed through an eyelet on the sky-worker used to lift the weights and trailed behind the weights as they fell. Prior to attaching the line it was found that spheres rotated as much as 90 degrees before impacting. This procedure assured essentially vertical impact of the accelerometer.

16. Twenty-six spheres of different size and density were dropped on the ground surface at various heights and ranges from the first gage. The resulting ground motion was measured along the instrumented radial line. A tabulation of the tests conducted is given in Appendix B. The weights varied from 9 to 2275 lb and the drop heights from 5 to 50 ft. The radial range to the first gage station varied from 10 to 135 ft. All of the weights were dropped from a sky-worker (Figure 7) except the 2275-lb cast iron sphere which was lifted by a dragline. The heavier weights were released by burning the polypropylene lifting rope with a propane torch. The lighter weights were released manually. Except for slight drying out of the surface the impact zone remained in good condition during the tests.

17. Range and crater measurements were made immediately after each test and were radio-transmitted to the instrument van for voice recording on the magnetic tape. This served the dual purpose of retaining a complete permanent record of each test on FM tape and

Figure 7. Typical Test

avoided possible contradictions between field records and FM tape records. Figure 8 shows several typical craters which were formed during the tests.

Figure 8. Typical Craters

PART IV: ANALYSIS OF THE RESULTS

Data Reduction

18. One hundred and seven tests were conducted. Twelve channels of surface motion measurements were recorded on FM analog magnetic tape and recovered in the form of oscillograph records such as the one shown in Figure 9. The particle motion paths (Figure 10) of the two wave groups identified on Figure 9 exhibit typical Rayleigh-type wave characteristics for a layered system like the WES Site No. 2. The first wave group arrivals exhibited retrograde particle path motion and had an average group velocity, V_{r1}, of 565 fps. The particle motion path of the second wave group considered was prograde-elliptical and its average group velocity V_{r2} was 265 fps. The peak to peak particle velocity amplitude and period was manually tabulated for each record. The group velocities were measured on each record and tabulated. The range, height of drop, weight, diameter, crater depth, and crater diameter were added to this compilation of raw data. The analog to digital conversions of the spheres deceleration pulses during impact were made on a high speed analog to digital converter at WES at a digitizing rate of 6 kHz. The digital data were then processed through a Honeywell 400 digital computer produced magnetic plot tapes for an off-line plotter. Typical results of this procedure are shown in Figure 11. The peak acceleration a_p and duration T_d were included in the raw data bank. The rebound of the spheres, which is illustrated by the second peak in Figure 11, was considered insignificant.

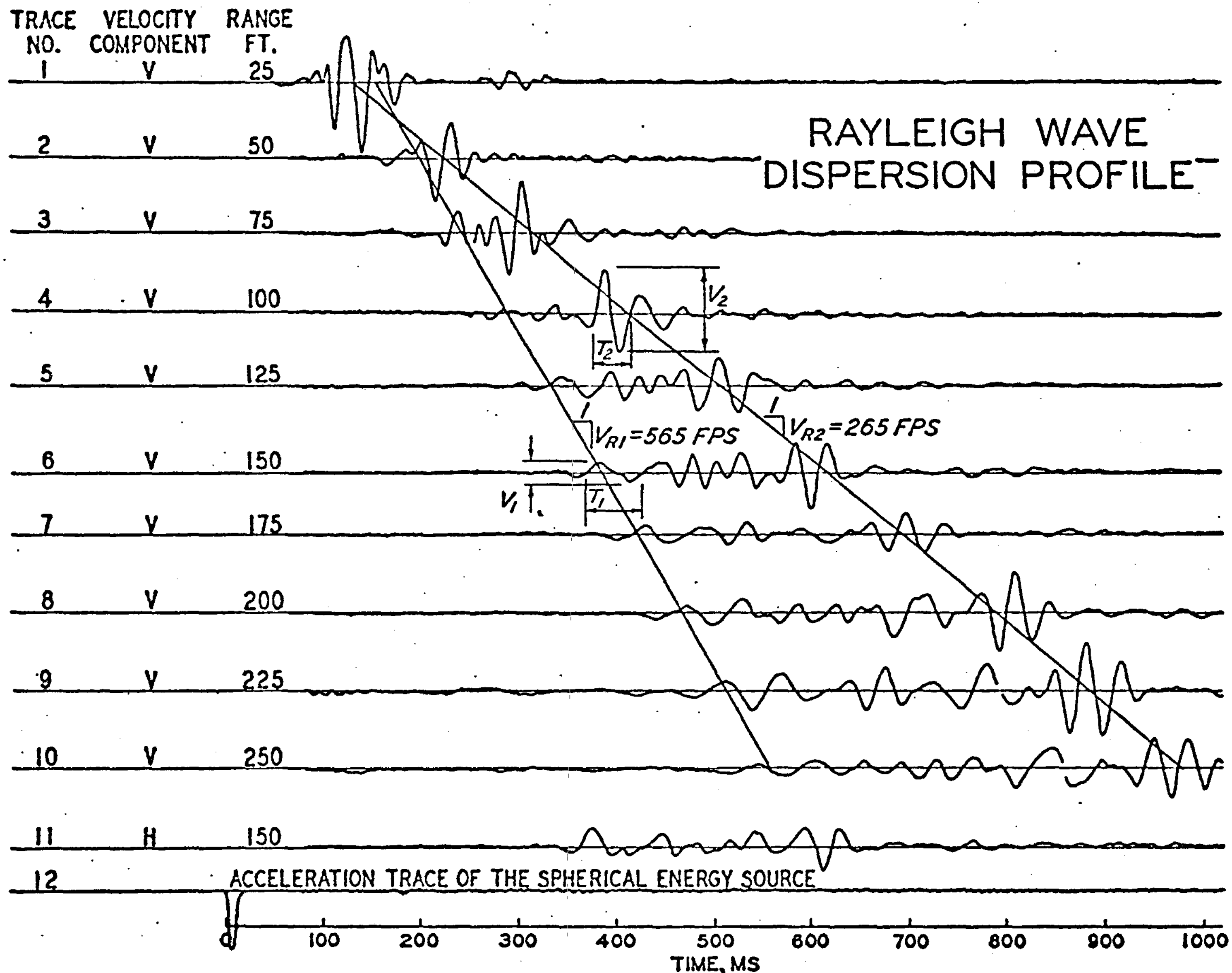

Figure 9. Typical Raw Data Record

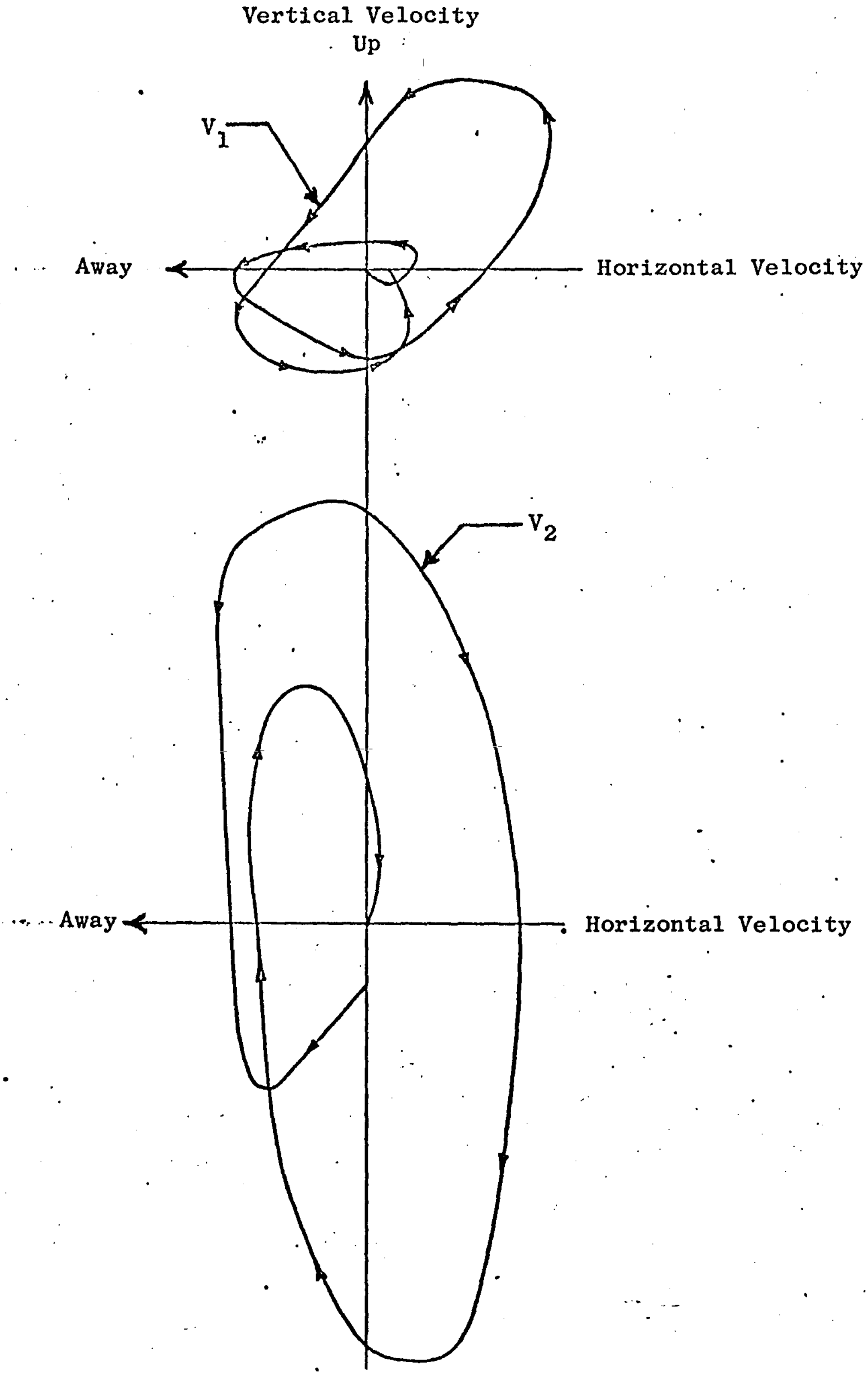

Figure 10. Particle Motion Paths

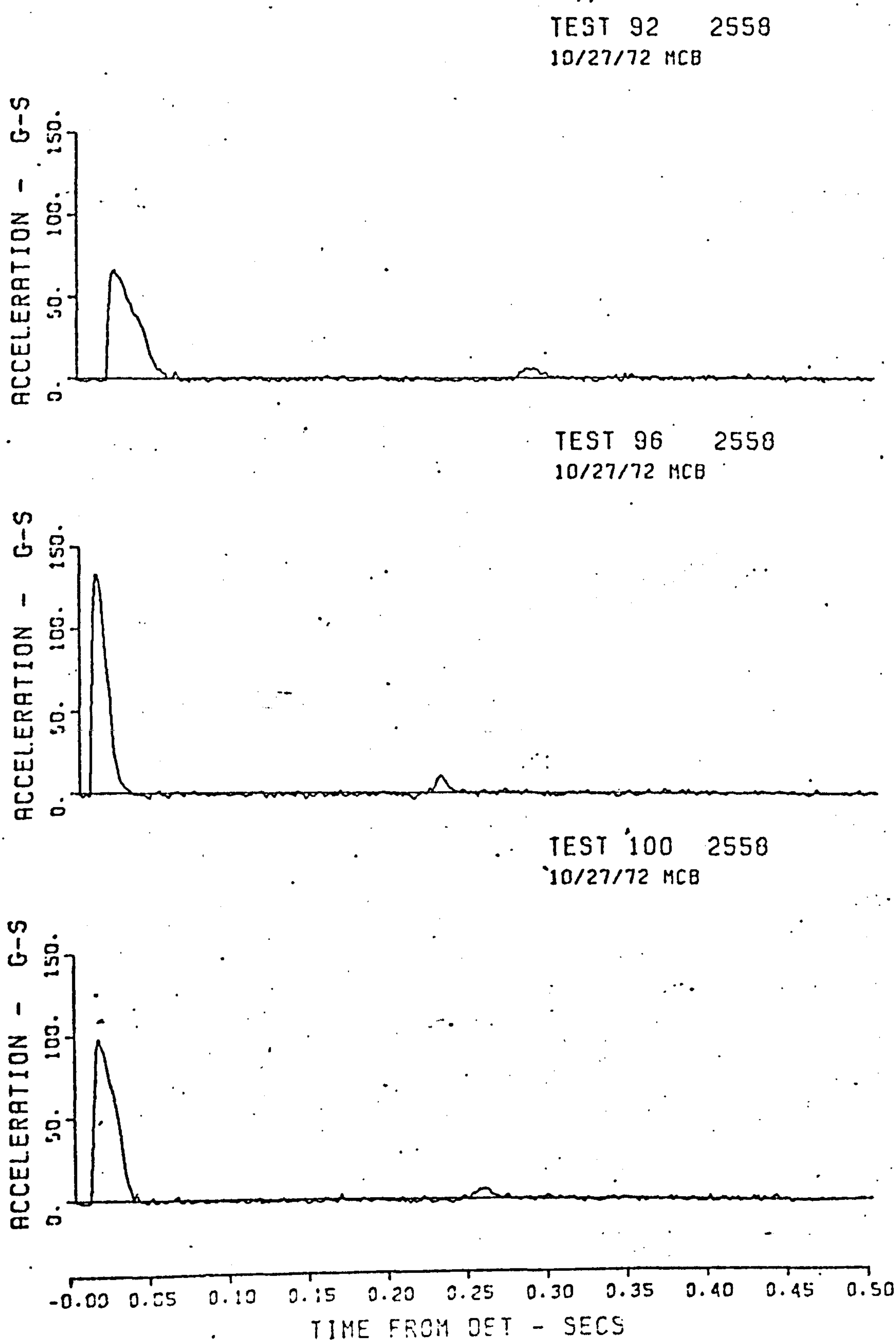

Figure 11. Typical Sphere Accelerations, g

Method of Analysis

19. A computer program was written to compute the Pi-terms contained in the general functional relationship previously derived (Equation 1). This operation established a data bank consisting of approximately 12,000 dimensionless data bits to be used in the analysis.

Equations presented in this report were derived by a least-squares linear-regression method. The program was designed to fit the "best fit" least-squares line through the linear transform of the six equations below:

$$Y = A + BX$$

$$Y = (A)^{BX}$$

$$Y = A(X)^{R}$$

$$Y = A + B/X$$

$$Y = 1/(A + BX)$$

$$Y = X/(A + BX)$$

where

Y = dependent variable

X = independent variable

A and B are constant and a correlation coefficient C was generated as a measure of "goodness of fit." C = 1 was a perfect correlation.

21. All of the data were analyzed on the WES GE 400 Computer Time Sharing System and all plotting was done on-line with a

Hewlett Packard 7200A Graphic Plotter with the exception of the sphere deceleration data. A library program, Store and Manipulate (SAM), was extremely valuable in sorting and extracting pairs of data from the 12,000-bit data bank.

22. When the correlation coefficient was greater than 0.60, it was arbitrarily decided that the data had a sufficiently good fit to a straight line of the linear transform of the equation. The relatively simple statistical methods used for this report do not take full advantage of the massive amount of data which is generated by this test procedure. However, there was insufficient funding to collect soil parameter data and then run a stopwise multi-regression analysis to determine the influence of a third, fourth, etc., property upon the original pairs. The procedure used is a "shotgun" approach in that two parameters were selected and plotted against each other. It is hoped that funds will ultimately be available to permit refinements in the analysis of the available data.

Empirical Equations Developed

23. The total impulse or integrated force-time history of the cratering induced energy is one of the most important parameters needed to predict ground motions accurately, but also one of the most difficult to define quanitatively for explosions. In this study the deceleration of the spherical mass during impact is directly proportional to the total force acting on the ground surface. The action of the force during a finite interval of time is given by the

integral

$$\frac{W}{g} \int_{t_o}^{t_f} a(t)\, dt = \frac{W}{g} (v_f - v_o) \qquad (2)$$

where

v_o = initial velocity of the sphere = 0

v_f = impact velocity of the sphere = $\sqrt{2gH}$

The integral on the left is the linear impulse and the right side is the corresponding change in linear momentum. Obviously from Figure 11 there is only a slight amount of rebound (or residual momentum) after the initial impact. Thus, the impulse imparted to the ground during initial impact is essentially equal to the product of the sphere's mass and impact velocity. Therefore

$$\int_{o}^{T_d} a(t)\, dt = \sqrt{2gH} \qquad (3)$$

Let

$dt = T_d\, d\tau$ and $a(t) = a_p\, F(\tau)$

where T_d is the deceleration pulse duration, a_p is the peak deceleration and τ is a generalized coordinate, then Equation 3 can be written

$$a_p\, T_d \int_{o}^{1} F(\tau)\, d\tau = \sqrt{2gH}$$

or

$$\sqrt{2gH}/a_p T_d = \int_o^1 F(\tau)d\tau \qquad (4)$$

A plot of the potential energy of the seismic source versus the dimensionless parameter defined in Equation 4 indicates that statistically (Figure 12)

$$a_p T_d/\sqrt{2gH} = 1.85 \qquad (5)$$

for all sources regardless of energy level or sphere geometry. Therefore, there exists a characteristic force-time function, $F(\tau)$, for this particular test site and method of creating a seismic source. If indeed there exists such a characteristic force-time function for any given test site, then it is possible that a good seismic descriptor which is easily measured has been discovered.

24. Assuming that the nonconservative forces such as kinetic friction are neglible, then the energy transmitted to the ground can be expressed as

$$W(H + C_d) = W/g \int_o^{C_d} a(x)\ d(x) \qquad (6)$$

where C_d is the crater depth. If $H >> C_d$, $x = C_d\eta$ and $a(\eta) = a_p G(\eta)$ then Equation 6 can be approximated by the expression

$$H/C_d = a_p/g \int_o^1 G(\eta)\ d\eta$$

73652

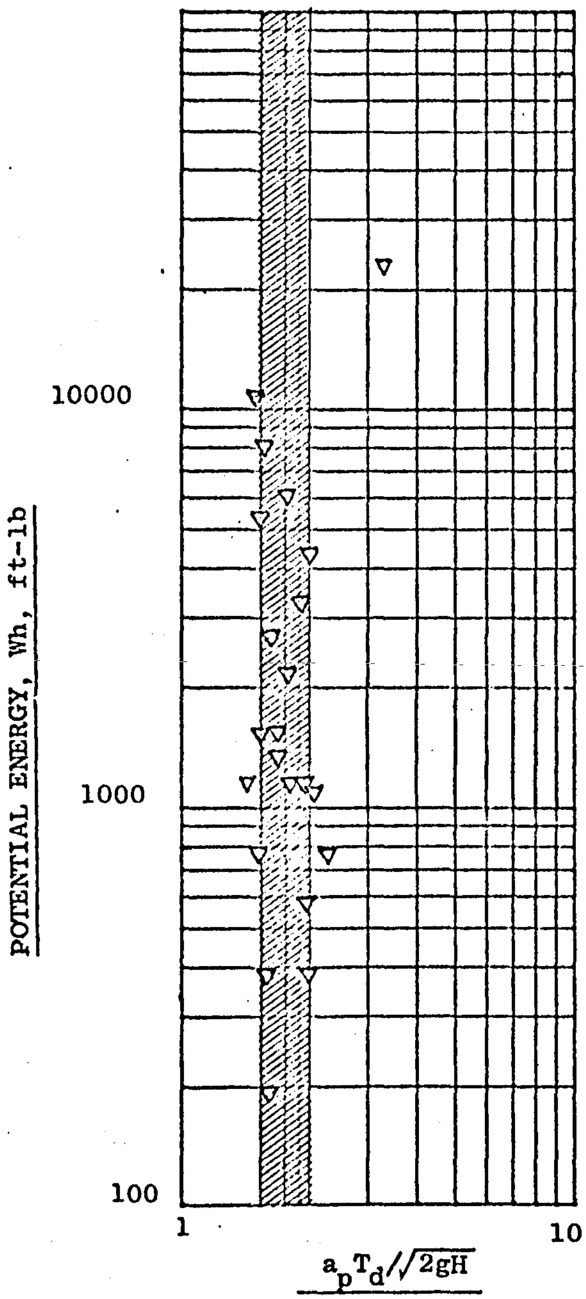

Figure 12. Normalized peak acceleration of the spheres during impact as a function of energy level

where η is a generalized coordinate. A plot of the dimensionless parameters H/C_d and a_p/g is shown in Figure 13. The "best fit" equation is a linear function defined as follows.

$$a_p/g = 0.95\ H/C_d \qquad (7)$$

Solving Equations 5 and 7 for H and equating the results yield the following relationship.

$$C_d/a_p(T_d)^2 \doteq 0.135 \qquad (8)$$

24. The kinetic energy of a missile during impact is partitioned into work to form the crater, to waste heat, and to kinetic energy of the ejecta. In this study the work done to form the crater is essentially equal to the kinetic energy of the sphere. The energy losses due to heat and ejecta were neglible due to the low impact velocities. The crater dimensions are obviously a function of the kinetic energy, the impacted media, the sphere diameter and possibly the sphere density. The same site was used for all tests to eliminate the effect of the impact media All of the craters formed were spherical segments which can be uniquely described by the measured crater depth C_d and crater radius C_r. Figure 14 summarizes the results of the correlation between the potential energy and the crater dimensions. The following equations resulting from the linear-regression analysis gives the crater depth and crater diameter a power function of potential energy when $C_d \leq C_r$.

$$C_d = 0.00661\ (WH)^{0.45} \qquad (9)$$

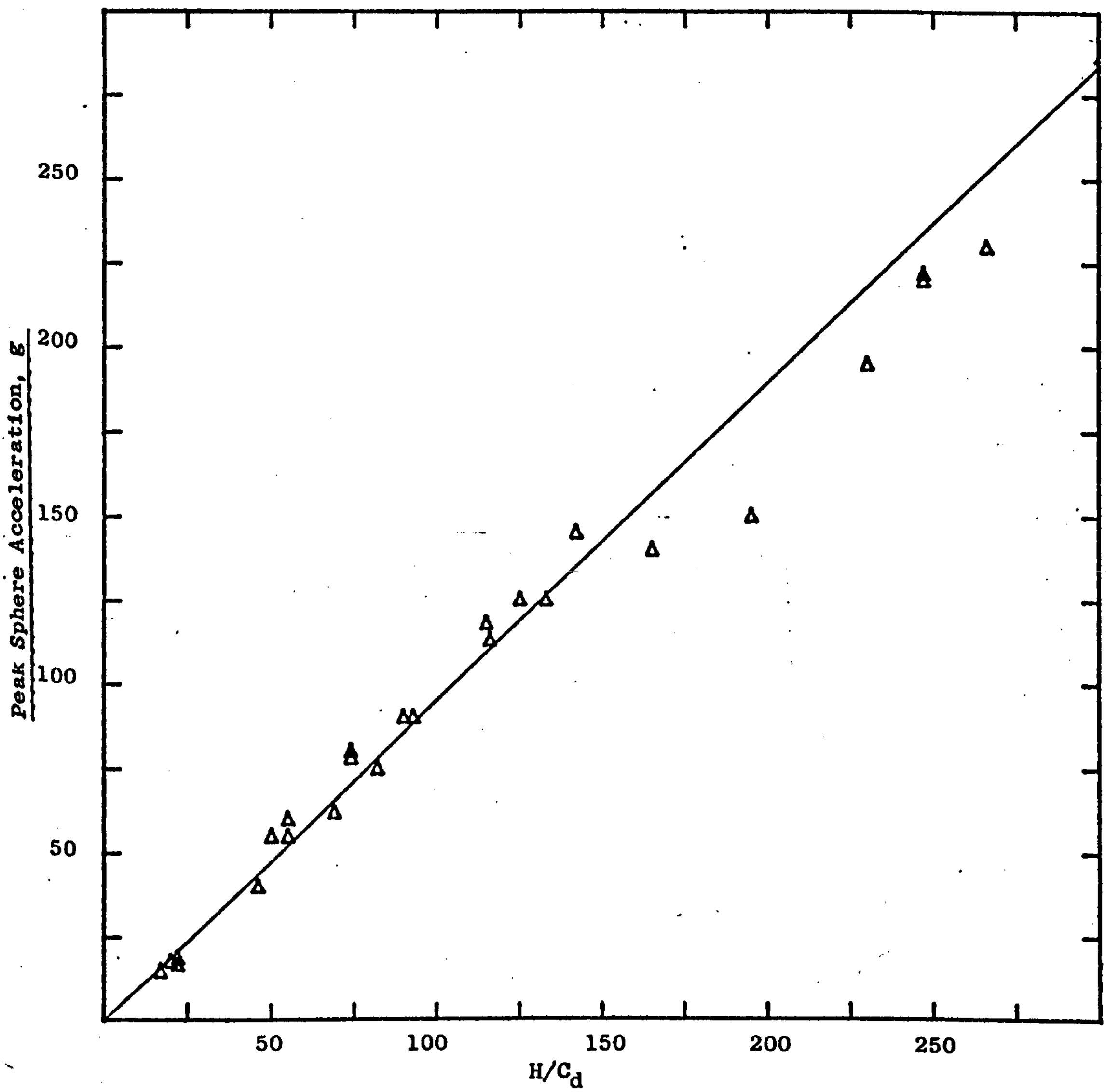

Figure 13. Normalized peak acceleration as a function of normalized crater depth

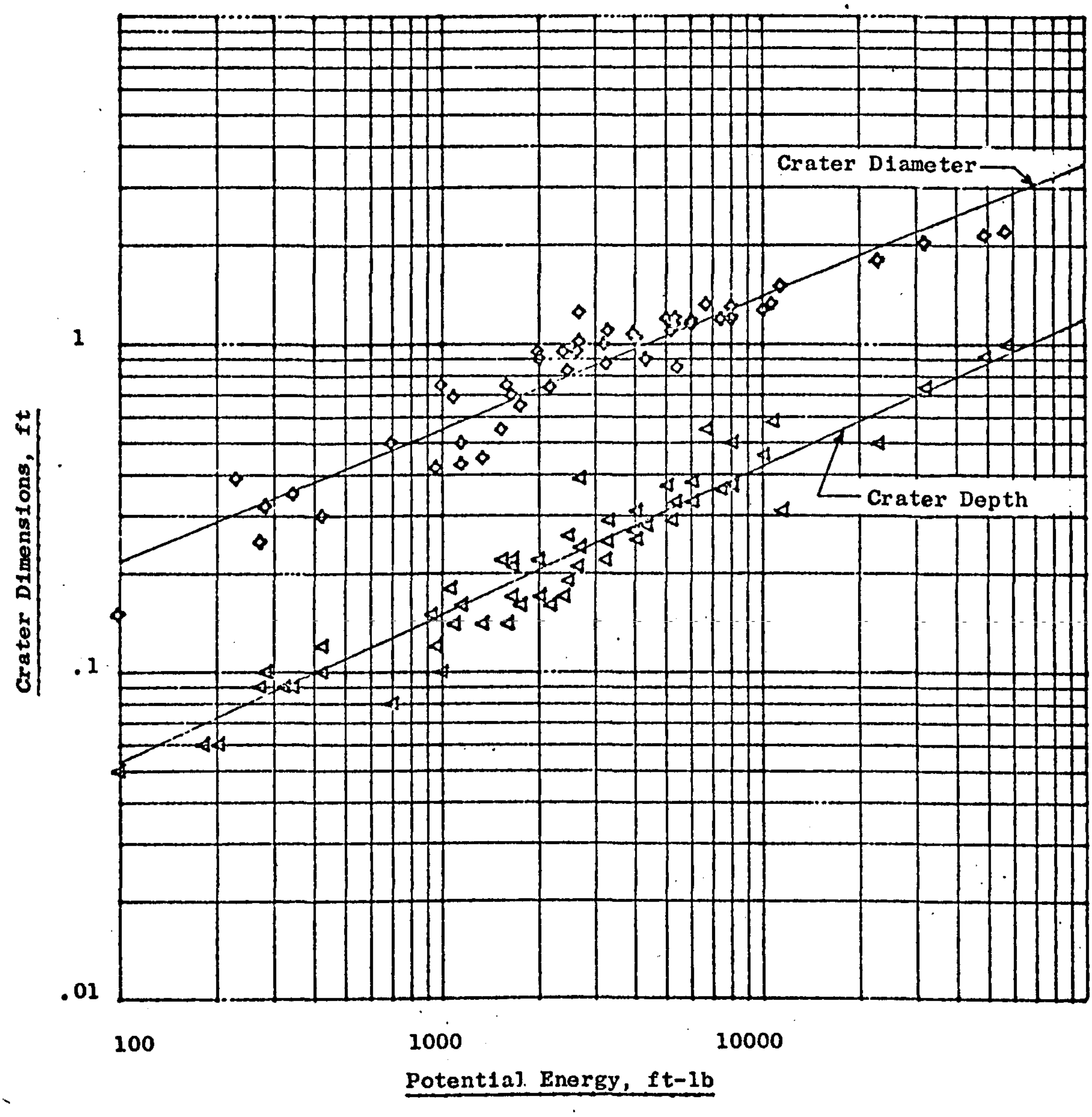

Figure 14. Crater dimensions as a function of energy level

$$C_r = 0.0168\ (WH)^{0.40} \qquad (10)$$

The diameter of the sphere is a unique function of the crater dimensions.

25. A normalized plot of the average vertical stress as a function of normalized time is shown in Figure 15. The stress was normalized by the peak stress σ_p for each test. The time, t, was normalized by the duration of the deceleration pulse T_d. The following exponential decay equation was obtained from the "best fit" analysis.

$$\frac{\sigma}{\sigma_p} = 1.25e^{-2.75t/T_d} \qquad (11)$$

26. The seismic response resulting from an excitation caused by an energy source such as the falling spherical weights used in this study was a very complex analog signal (Figure 9). To model the total signal analytically or empirically is an impossible task, however prominent features such as first wave and peak wave amplitudes, periods and wave group velocities can be used to characterize the ground motion. The seismic descriptors identified on Figure 9 were used to characterize the ground motion. The independent variables were energy level, energy density, and range from the source. The statistically significant correlations are presented in Appendix C in the form of data bands. The bandwidth was arbitrarily established to cover an estimated seventy to eighty percent of the data, but the prediction

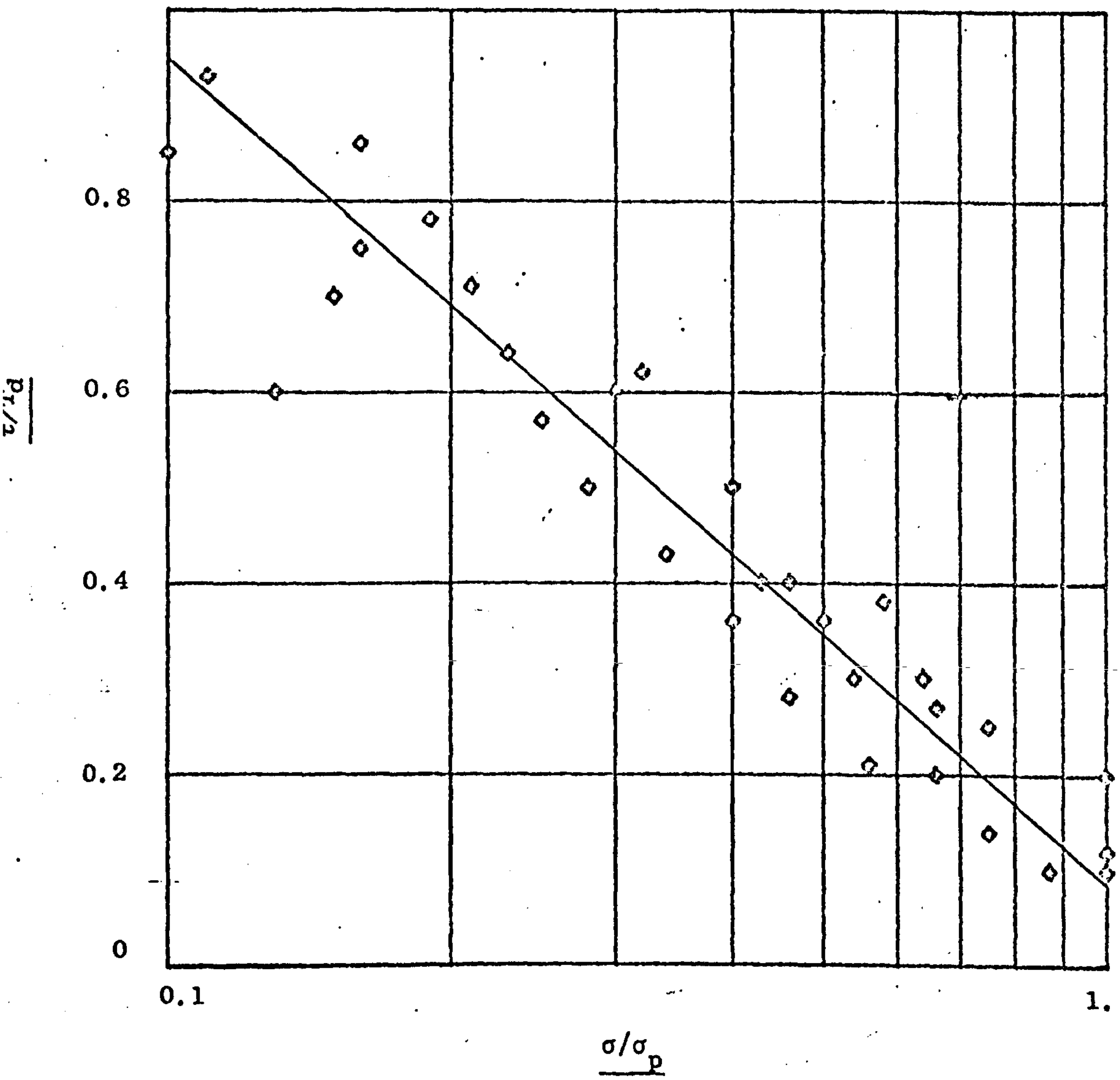

Figure 15. Normalized stress as a function of normalized time

equations were obtained from a linear-regression analysis of the complete data field consisting of approximately one thousand data pairs for each correlation. The following equations are the result of the "best fit" analysis.

$$(V_2T_2)/R = 0.026 \left\{(WH)/(\gamma R^4)\right\}^{0.625} \quad (12)$$

$$(V_2)^2/(gR) = 0.025(WH)/\gamma R^4) \quad (13)$$

$$(WH)/(\gamma R^4) = 0.0025 \left\{R/V_{r2}T_2)\right\}^{-4.5} \quad (14)$$

$$(V_1T_1)/R = 0.0042 \left\{(WH)/(\gamma R^4)\right\}^{0.58} \quad (15)$$

$$(WH)/(\gamma R^4) = 0.000183 \left\{R/(V_{r1}T_1)\right\}^{-5.6} \quad (16)$$

These equations reflect the gross effect of the normalized energy level and the normalized seismic parameters. Physically the normalized seismic parameters can be interpreted as: (a) $(VT)/R$ is a normalized particle displacement, (b) V^2/gR is a normalized particle kinetic energy, and (c) V_rT/R is a normalized Rayleigh wavelength. Typical data from three tests are presented in Figures 16, 17, and 18.

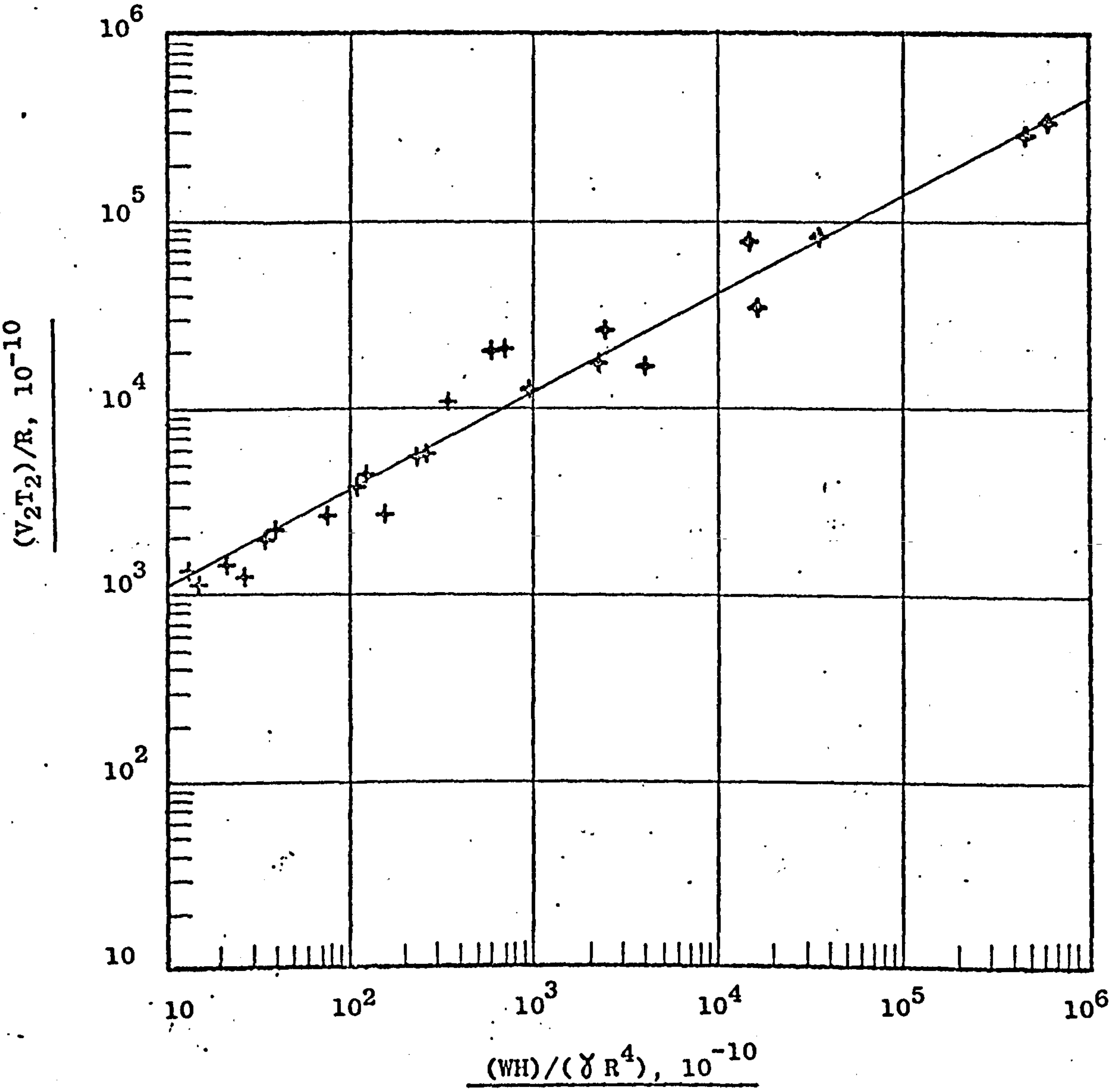

Figure 16. Normalized particle displacement as a function of normalized potential energy

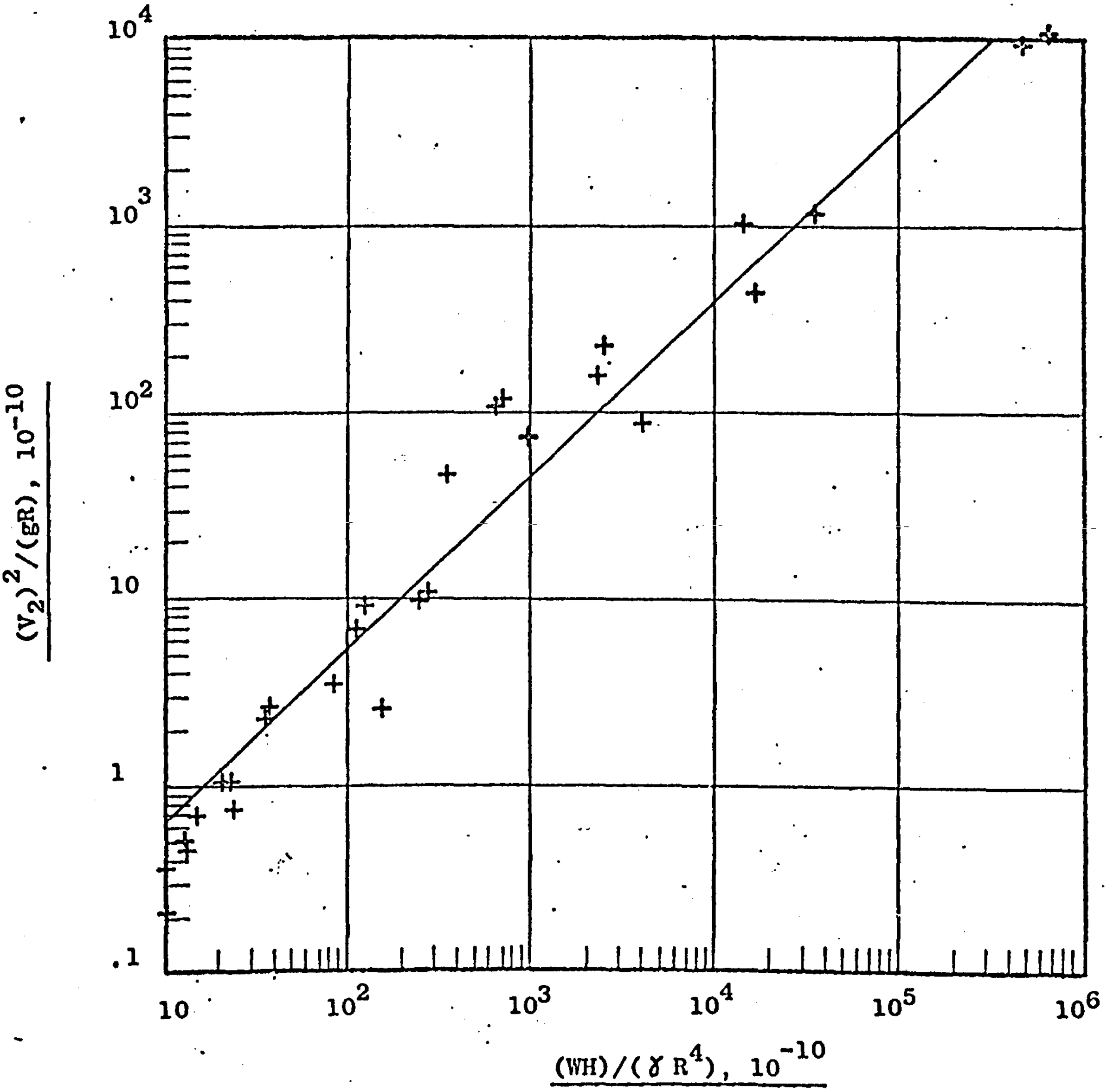

Figure 17. Normalized peak particle kinetic energy as a function of normalized potential energy

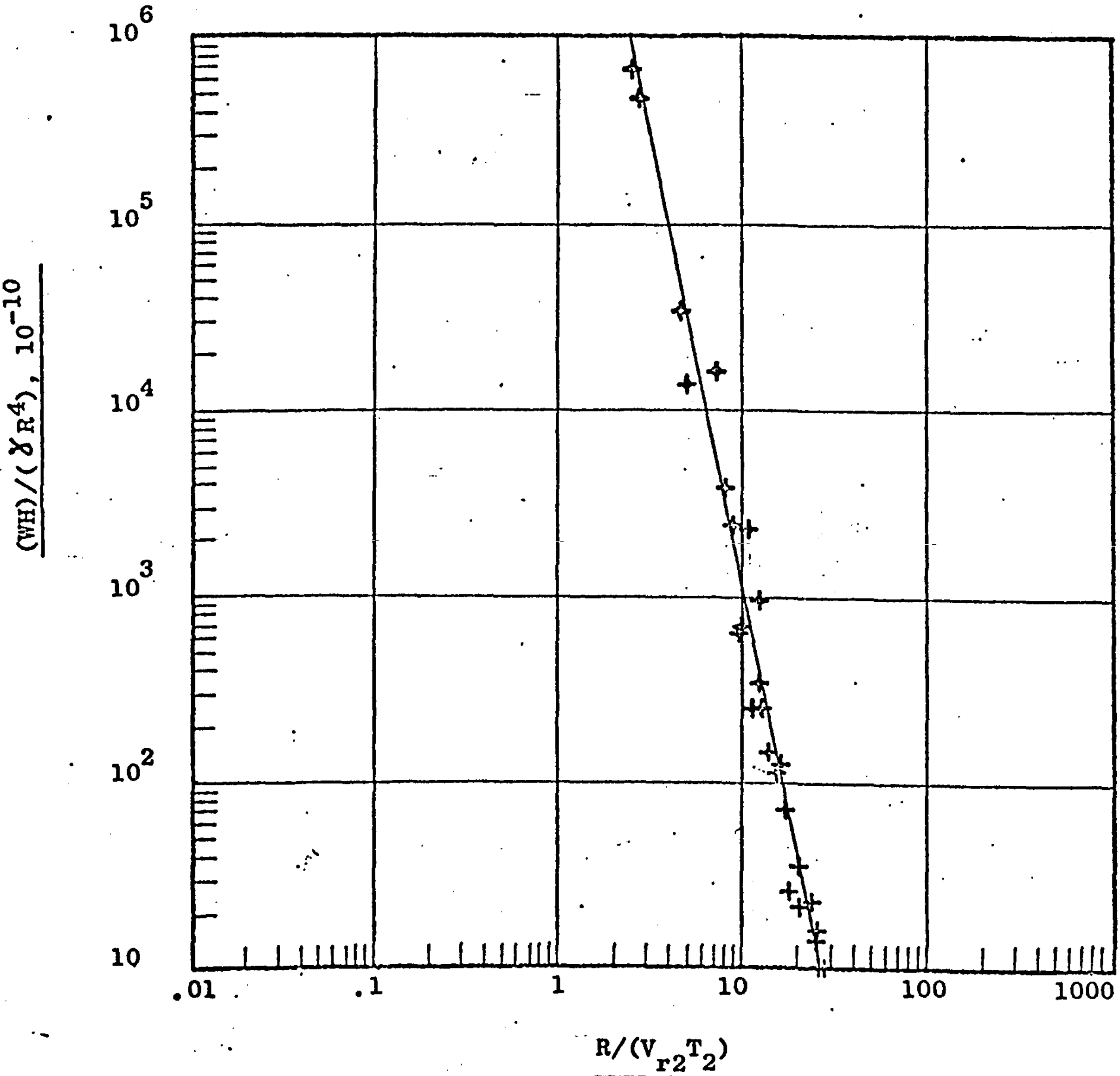

Figure 18. Normalized potential energy as a function of normalized peak Rayleigh wavelength

PART V: CORRELATIONS BETWEEN HIGH EXPLOSIVE DATA AND IMPACT PREDICTION EQUATIONS

Introduction

27. The results of the impact tests indicate that this technique can be used to determine some characteristic properties for a particular geological site. Prediction equations for the force-time history of the seismic energy source, crater dimensions and several characteristic seismic response discriptors were developed for this particular test method and site. As a result of the statistically favorable findings, consideration was given to the possible use of the technique as a model to predict far-out (Raleigh) motions and crater dimensions for high explosives. High explosive data for the site used for the impact study were not available, hence it was necessary to use high explosive data from sites grossly different from the impact study site. However, if the impact prediction equations are truly characteristic of the phenomena then the resulting correlations with HE data will still be valid, but will include a media properties distortion function, i.e., similitude requirements on media properties have been violated.

Peak Vertical Particle Velocity

28. The peak to peak vertical particle velocity in Equation 13 can be expressed as peak vertical velocity as a function of range in feet and seismic energy level in lb-TNT by assuming an energy equivalence of 1.41×10^6 ft-lb/lb-TNT. The result of this conversion

yields

$$V_i = 50(E/R^3)^{1/2} \tag{17}$$

where

V_i = $\pm$ peak vertical particle velocity for impacts in ft/sec

E = yield energy in lb-TNT

R = range from source in ft

High explosive peak vertical velocity data, V_e, in the region dominated by surface waves (Rayleigh) is limited. However a recent 500-ton TNT event, MIXED COMPANY, included 13 channels of vertical velocity data at ranges from 1400 ft to 18,000 ft. Two other 500-ton TNT events, PRAIRIE FLAT and DIAL PACK, included several vertical velocity gages in the far-out region. The ratio of the explosive versus impact vertical velocity is shown in Figure 19. The peak velocity, V_i, was computed from the equation given above. From Figure 19 this yields

$$V_e = 0.25V_i \tag{18}$$

or in terms of energy level and range, the explosive peak vertical particle velocity is given by

$$V_e = 12.5\ (E/R^3)^{1/2} \tag{19}$$

in the far-out region dominated by Rayleigh waves.

Predominant Frequency

29. The predominant frequency for the peak vertical velocity was derived from Equations 12 and 13 with the same assumptions

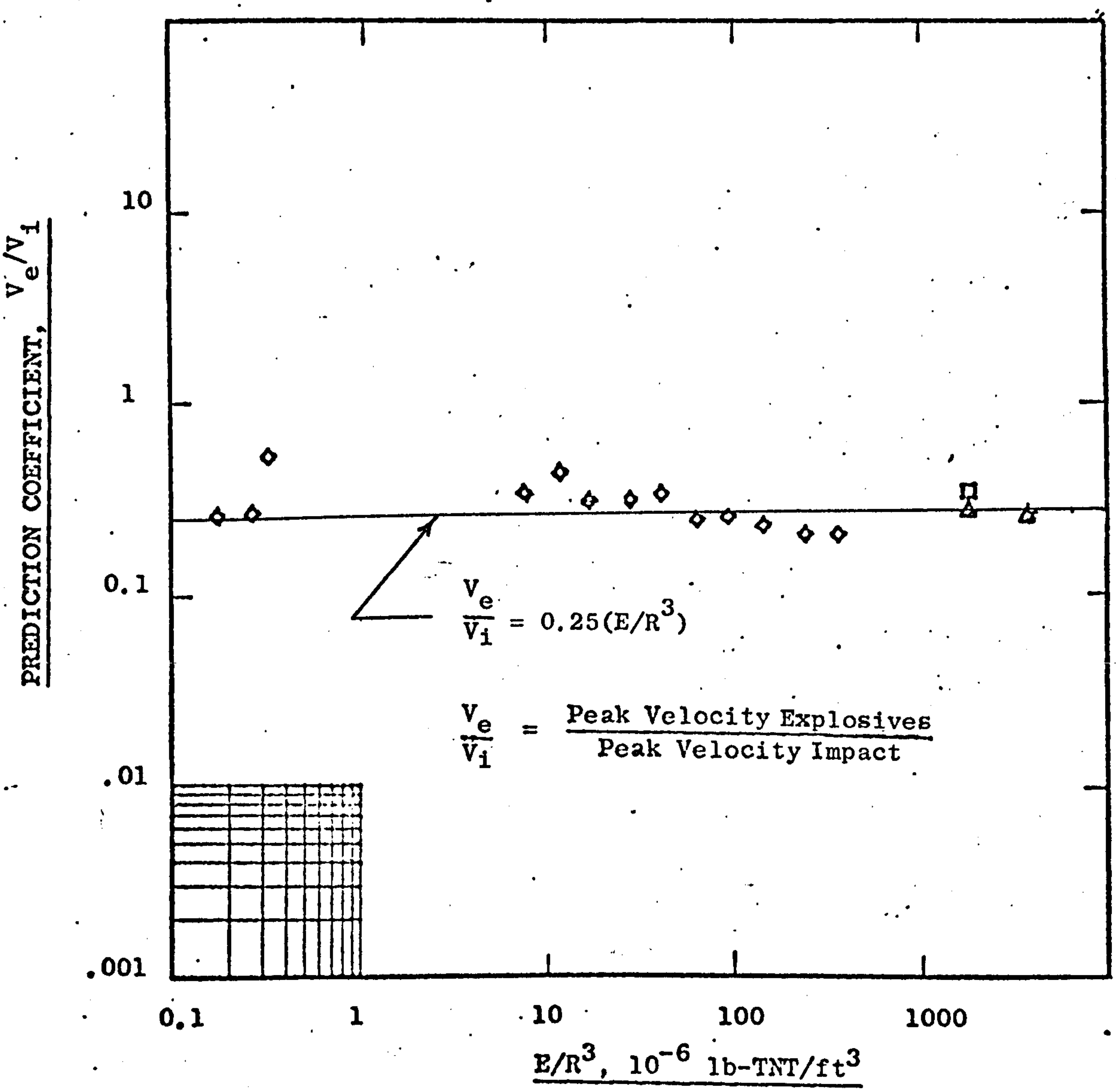

Figure 19. Ratio of peak velocity caused by explosions and impact as a function of normalized energy level

used to obtain the peak velocity equation. The period, T_i , in seconds for the impact study is obtained from Equations 12 and 13

$$T_i = 0.1 \ (E)^{1/8} \quad . \tag{20}$$

and the predominant frequency, F_i , in Hz equals $1/T_i$, thus

$$F_i = 10 \ (E)^{-1/8} \tag{21}$$

The dominant frequency for the MIXED COMPANY high explosive event was 6 Hz in the far-out region and 1 to 2 Hz for PRAIRIE FLAT and DIAL PACK events. The important conclusion is the weak dependency of frequency with energy and zero dependency with range.

Crater Dimensions

30. The impact crater dimensions in terms of lb-TNT equivalent can be obtained from Equations 9 and 10. The conversion from ft-lb energy to lb-TNT equivalent implies that the crater radius and crater depth for impact can be expressed as follows:

$$(C_r)_i = 4.86 \ (E)^{0.40} \tag{22}$$

and

$$(C_d)_i = 3.86 \ (E)^{0.45} \tag{23}$$

Craters from HE events are normally expressed in terms of apparent crater dimensions and true crater dimensions. Since the impact crater dimensions were not influenced by an ejecta plume it was assumed that the best correlation ratio was the true crater dimensions. A statistically significant number of half buried (HOB = 0) HE tests were conducted in moist lascustrian silt at the NTS (Reference 1). This type of material is reasonably similar to the impact test site. The HE yields ranged from 1 to 40,000 lb-TNT. The ratio of true HE crater dimensions to impact crater dimensions computed from Equations 21 and 22 are shown in Figure 20 and 21. Then

$$(C_{rt})_e = 0.28\ (E)^{-0.1}\ (C_r)_i \tag{24}$$

$$(C_{dt})_e = 0.23\ (E)^{-0.15}\ (C_d)_i \tag{25}$$

or in terms of energy yields the prediction equations for true HE craters are as follows:

$$(C_{rt})_e = 1.35\ (E)^{0.31} \tag{26}$$

$$(C_{dt})_e = 0.85\ (E)^{0.30}$$

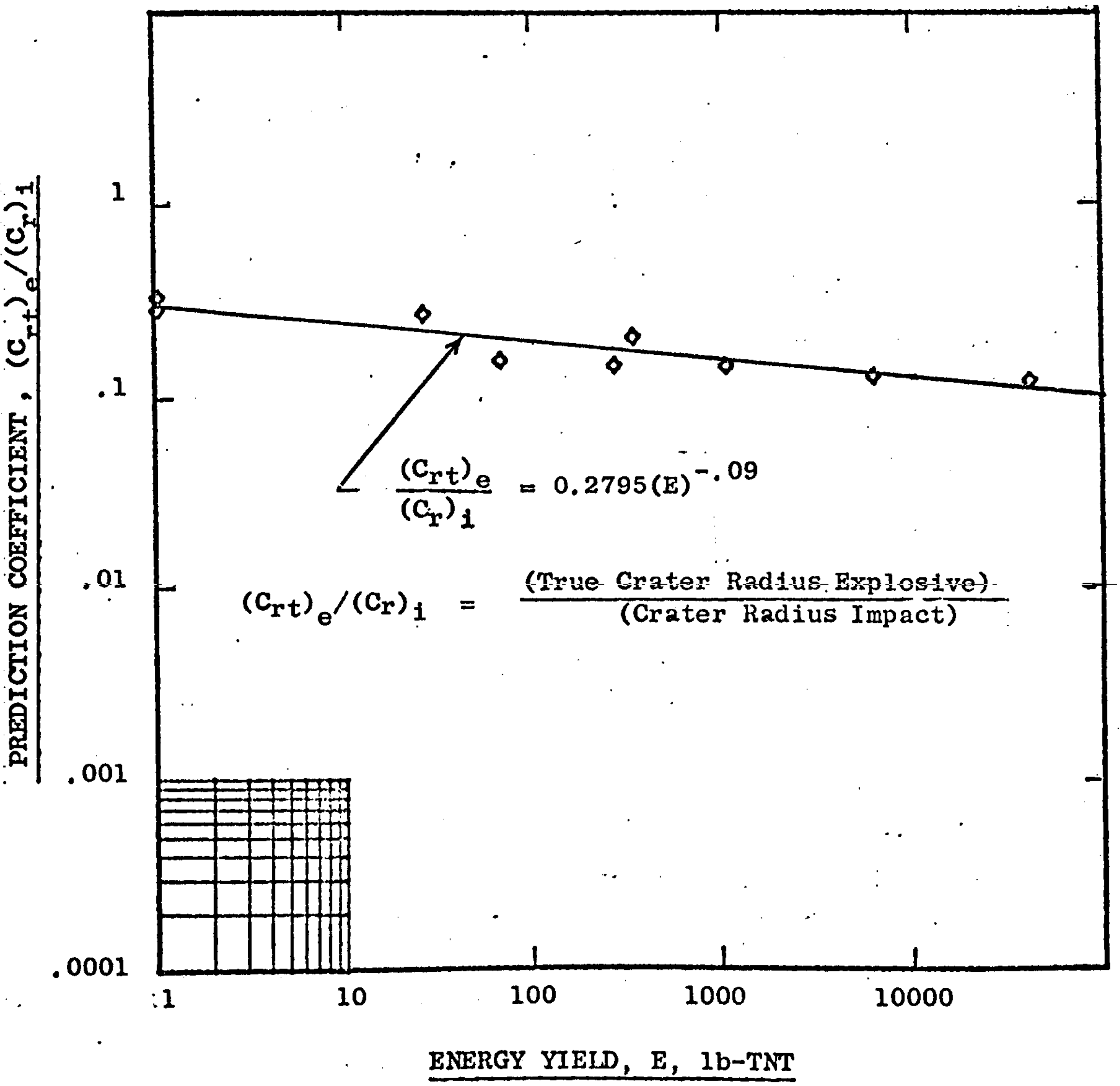

Figure 20. Ratio of true crater radii caused by zero HOB explosions and impacting spheres as a function of energy level

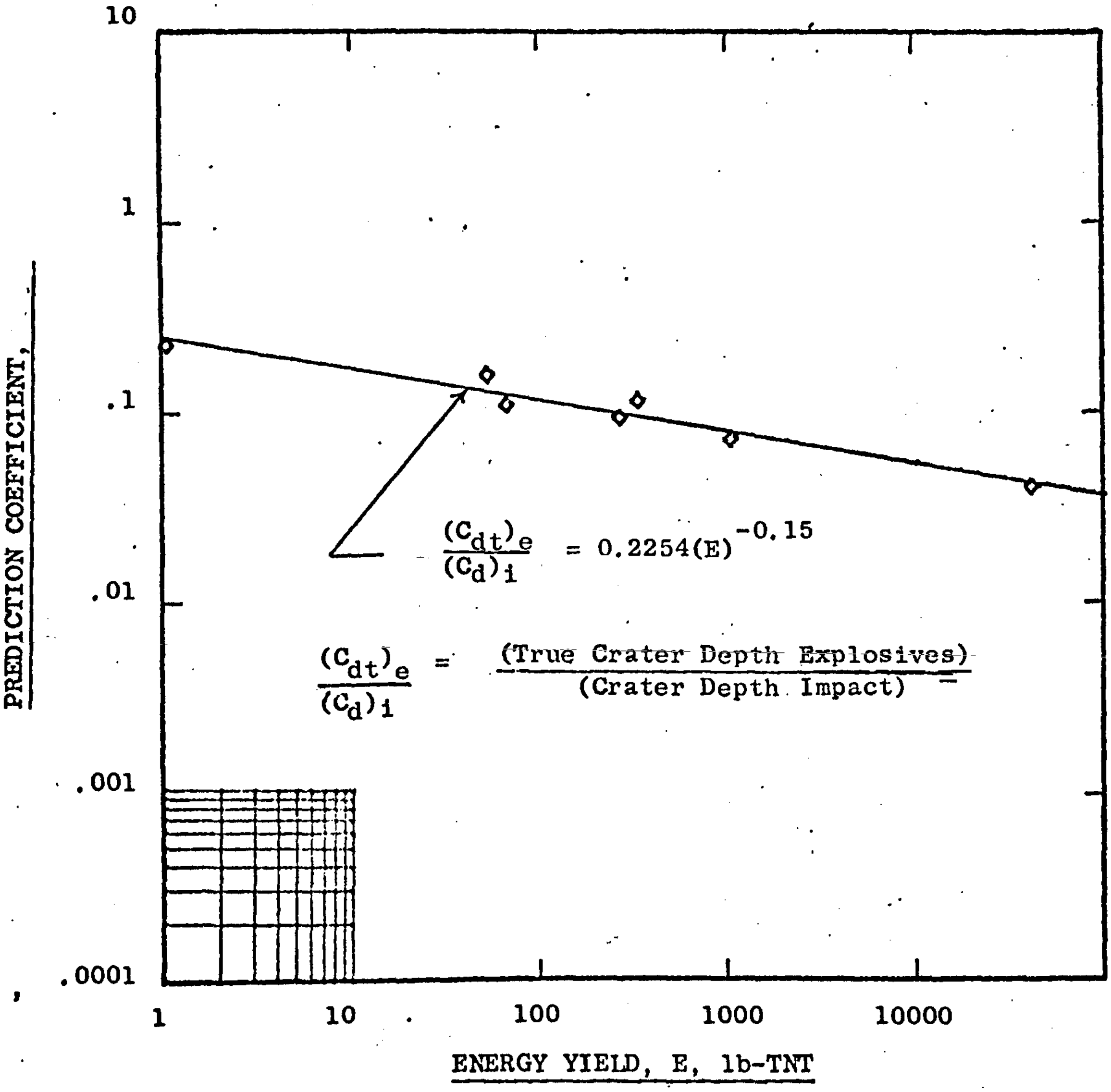

Figure 21. Ratio of true crater depths caused by zero HOB explosions and impacting spheres as a function of energy level

PART IV: CONCLUSIONS AND RECOMMENDATIONS

Conclusions

31. The results of Spherical Mass Impact Technique tests conducted to date indicate that the technique will provide useful information on Rayleigh waves. An effective means of realizing a controlled and variable energy source has been developed. Specifically, it has been demonstrated that:

a. The period of the predominant surface wave is weakly dependent upon the energy level, i.e., $E^{1/8}$ power.

b. The peak surface wave velocity is a function of the scaled energy level, $(E/R^3)^{1/2}$.

c. The true crater dimensions can be scaled with an effective energy level of approximately $E^{0.4}$.

d. There exists a one to one correspondence between impact and explosively created phenomena.

Recommendations

32. The technique developed here constitutes a firm basis for additional study, however actual application of the results should be used with caution. Additional tests at several different geological sites would be desirable, particularly at sites where explosive and impact tests could be conducted concurrently.

REFERENCES

1. Davis, K. L., and Carnes, B. L., "Cratering by Explosions: A Compendium and an Analysis," U. S. Army Engineer Waterways Experiment Station, TR No. (IN PROCESS OF BEING PUBLISHED).

2. Ingram, J. K., "Ground Motions and Stress Measurements Project LN-302 MIXED COMPANY EVENT," Project Officer's Report DNA No. (REPORT IN PREPARATION).

3. Caudle, W. N., "The Feasibility of Rapid Soil Investigations Using High-speed, Earth-Penetrating Projectiles," Proceedings International Symposium on Wave Propagation and Dynamic Properties of Earth Materials, Aug 23-25, 1967.

APPENDIX A

EQUIPMENT

APPENDIX A

Equipment

Item		Description		Location	Orientation
12	Particle velocity transducer	Geospace HS-10-1		1-6 & 8-11	Vertical
		Sensitivity, Mv/ips (rms)	7.5	7 & 12	Horizontal
		Damping, Percent	70		
		Natural frequency, Hz	1.0		
		Coil resistance, Ohms	4100		
1	Accelerometer	Endevco 2264 MI		Spheres	Vertical
		Sensitivity, P-P g's	10,000		
		Damping, Percent			
		Natural frequency, Hz			
12	DC Amplifiers	CEC 1-165		1-12	
1	Oscillograph	CEC 5-119		1-12	
1	Tape Recorder	Sangamo 3500		1-12	

* Signal conditioning circuit WES-calibration and balancing circuit.

APPENDIX B

TESTS CONDUCTED

APPENDIX B

Tests Conducted

Test No.	Weight lb	Diameter ft	Height ft	Range ft	Crater Diameter ft	Crater Depth ft	Potential Energy ft lb
1	28.5	0.81	12.0	50			342
2	10.0	0.59	12.0	50			120
3	28.5	0.81	6.0	10			171
4	10.0	0.59	6.0	10			60
5	16.0	0.59	6.0	10			96
6	21.0	0.59	6.0	10			126
7	9.0	0.49	6.0	10			48
8	28.5	0.81	10.0	30			285
9	16	0.81	10.0	30			160
10	10	0.59	10.0	30			100
11	16	0.59	10.0	30			160
12	21	0.59	10.0	30			210
13	9	0.48	10.0	30			90
14	28.5	0.81	12.0	50			242
15	16.0	0.81	12.0	50			192
16	10.0	0.59	12.0	50			120
17	21.0	0.59	12.0	50			252
18	21.0	0.59	12.0	50			252
19	9.0	0.48	12.0	50			108
20	21.0	0.59	20	50		0.10	420
21	9.0	0.48	20	50		0.06	180
22	34.0	0.75	20	50			700
23	13.0	0.75	20	50			260
24	46.0	0.75	20	50		0.15	920
25	10.0	0.59	20	50		0.06	200
26	16.0	0.59	20	50		0.09	320

(continued)

APPENDIX B (cont'd)

Tests Conducted

Test No	Weight lb	Diameter ft	Height ft	Range ft	Diameter ft	Depth ft	Potential Energy ft lb
27	108.0	1.00	30	75	0.85	0.21	5400
28	54.5	1.00	30	75	0.73	0.17	1635
29	58.0	0.81	30	75	0.65	0.16	1740
30	81.5	1.00	30	75	0.83	0.19	2445
31	33.0	1.00	30	75	0.75	0.10	990
32	23.0	0.75	30	75	0.50	0.08	690
33	44.0	0.81	30	75	0.76	0.36	1320
34	54.5	1.00	30	50		0.22	1635
35	81.5	1.00	30	50		0.26	2445
36	35.0	0.75	30	50		0.18	1050
37	58.0	0.81	30	50		0.21	1640
38	44.0	0.81	30	50		0.14	1320
39	266.0	1.34	30	50	1.19	0.36	7980
40	200.0	1.34	30	50	1.18	0.38	6000
41	79.0	1.34	30	50	0.90	0.17	2370
42	131.0	1.34	30	50	1.08	0.27	3930
43	266.0	1.34	20	25	1.15	0.33	5320
44	200.0	1.34	20	25	1.10	0.31	4000
45	131.0	1.34	20	25	0.95	0.21	2620
46	79.0	1.34	20	25	0.75	0.14	1580
47	81.5	1.00	10	10			315
48	81.5	1.00	10	10			315
49	266.0	1.34	10	31	1.25	0.39	2660
50	11.38	0.50	30	10	0.35	0.09	341
51	14.0	0.34	30	10	0.30	0.10	420
52	7.0	0.27	30	10	0.25	0.09	270

(continued)

APPENDIX B (cont'd)

Tests Conducted

Test No.	Weight lb	Diameter ft	Height ft	Range ft	Crater Diameter ft	Crater Depth ft	Potential Energy ft lb
53	3.31	0.21	30	10	0.15	0.05	99
54	11.38	0.50	20	10	0.39	0.11	228
55	14.0	0.34	20	10	0.32	0.11	280
56	7.0	0.27	20	10			140
57	3.31	0.21	20	10			66
58	266.0	1.34	37.6	135	1.27	0.46	10001
59	200.0	1.34	37.0	135	1.19	0.36	7400
60	131.0	1.34	39.6	135	1.10	0.29	5188
61	79.0	1.34	40.3	135	1.00	0.22	3184
62	266.0	1.34	25.0	135	1.32	0.55	6650
63	200.0	1.34	25.0	135	1.20	0.37	5000
64	131.0	1.34	25.0	135	1.10	0.29	3275
65	79.0	1.34	25.0	135	1.00	0.22	1975
66	Vibrator test						
67	Vibrator						
68	Vibrator						
69	38.0	0.48	10	17.4	0.41	0.11	380
70	38.0	0.48	15	17.4	0.40	0.11	570
71	38.0	0.48	20	17.4	0.46	0.17	760
72	38.0	0.48	20	17.4	0.45	0.15	760
73	38.0	0.48	10	17.4	0.42	0.13	380
74	38.0	0.48	15	16.0	0.40	0.11	380
75	38.0	0.48	20	40.0	0.42	0.14	760
76	38.0	0.48	30	40.0	0.50	0.18	1140
77	38.0	0.48	30	40.0	0.46	0.18	1140
78	38.0	0.48	30	40.0	0.42	0.13	1140

(continued)

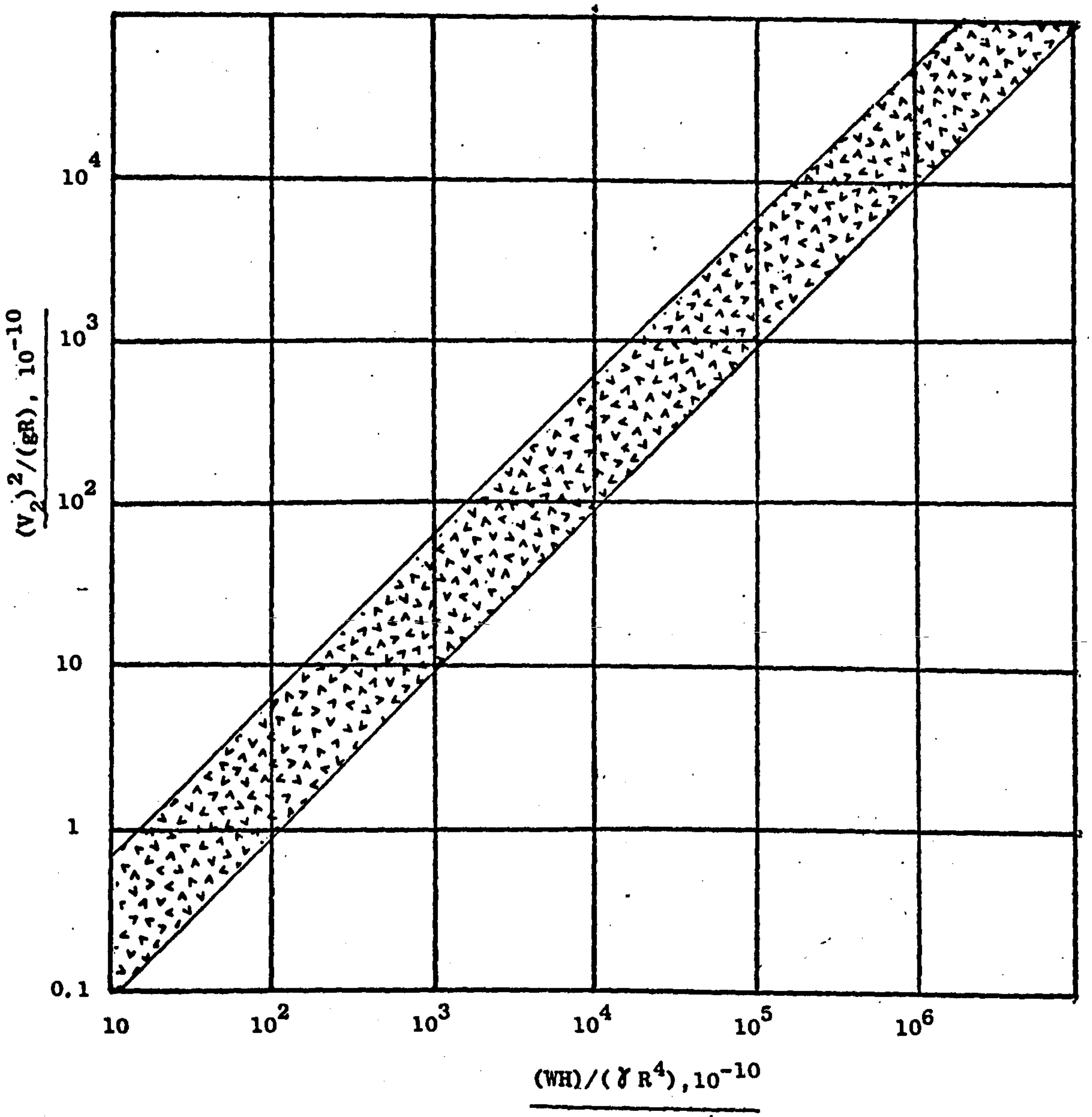

$(V_2)^2/(gR)$, 10^{-10}
10^4
10^3
10^2
10
1
0.1
10
10^2
10^3
10^4
10^5
10^6
$(WH)/(\gamma R^4)$, 10^{-10}

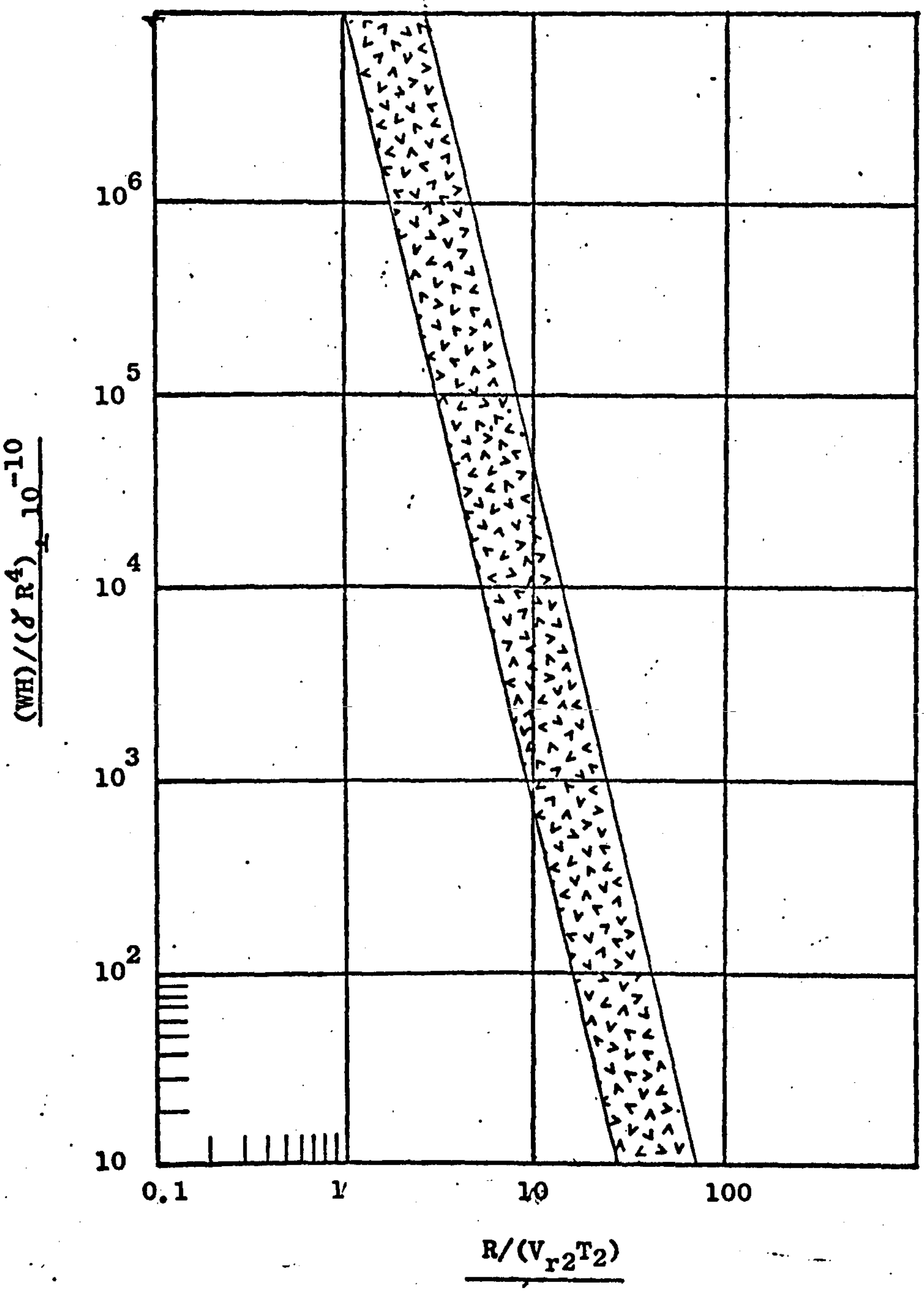

$(WH)/(\gamma R^4)_{\perp}\ 10^{-10}$
10^6
10^5
10^4
10^3
10^2
10
0.1
1
10
100
$R/(V_{r2}T_2)$

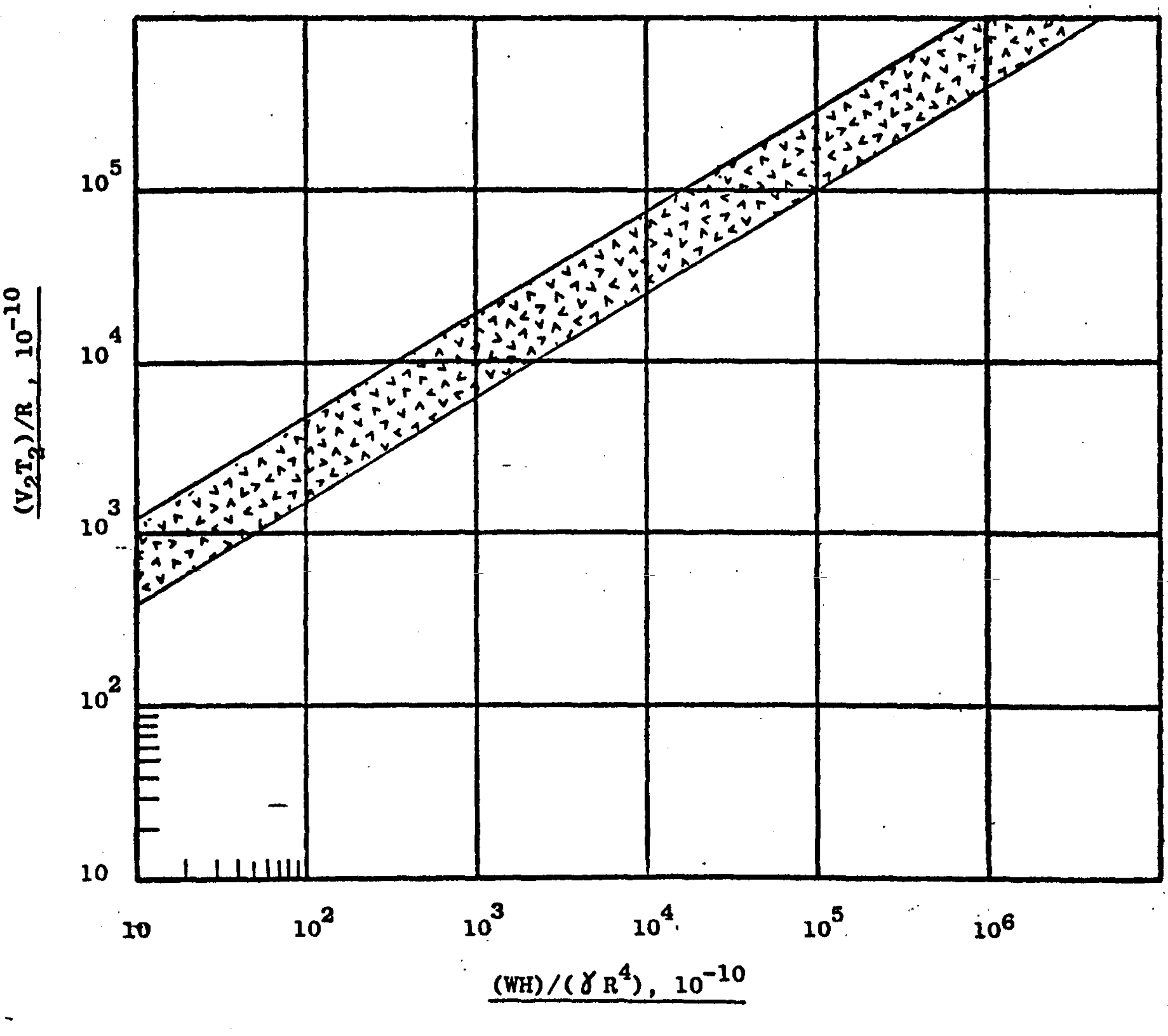
10
10^2
10^3
10^4
10^5
$(V_2T_2)/R$, 10^{-10}
10
10^2
10^3
10^4
10^5
10^6
$(WH)/(\gamma R^4)$, 10^{-10}

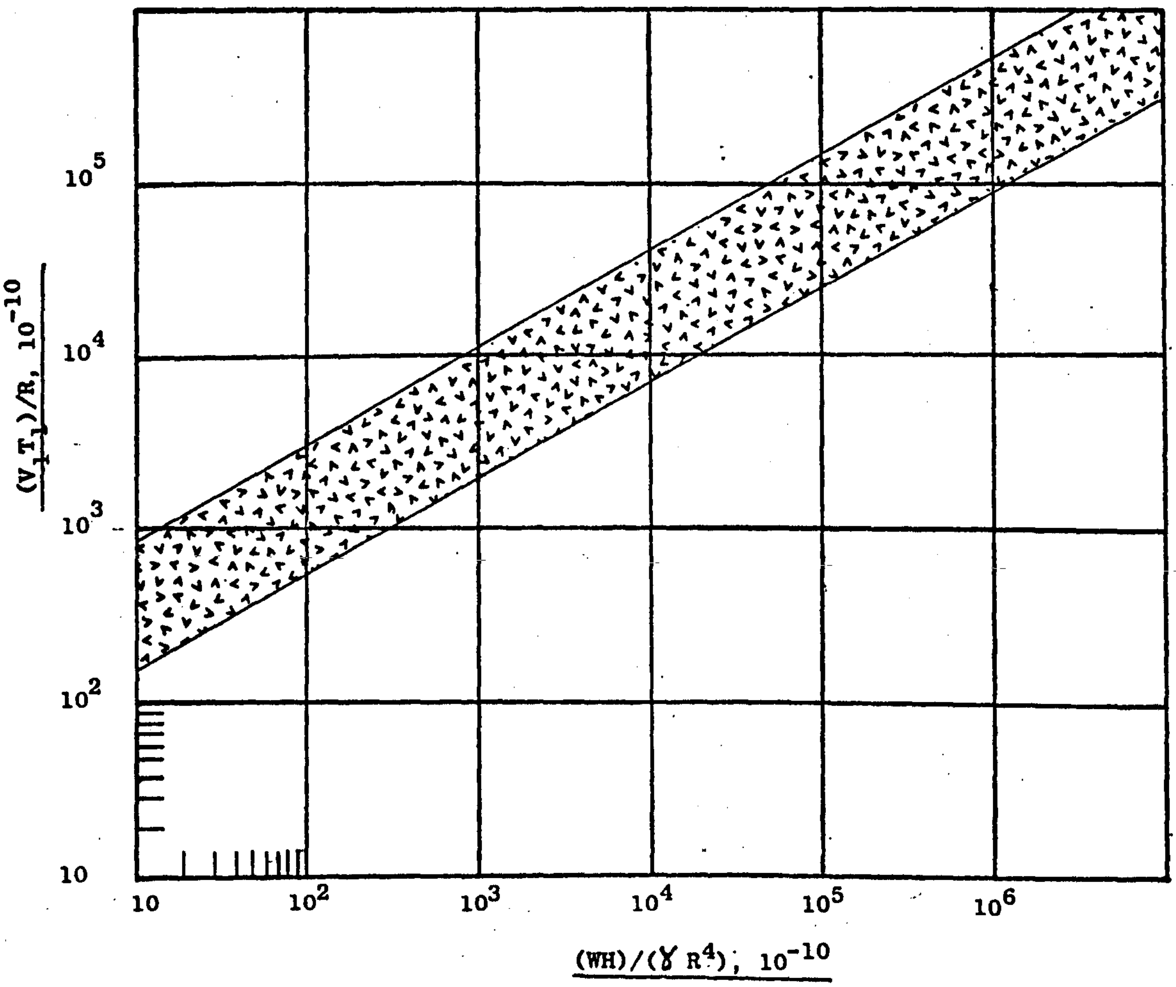

10^5
10^4
10^3
10^2
10
10
10^2
10^3
10^4
10^5
10^6
$(V_1T_1)/R$, 10^{-10}
$(WH)/(\gamma R^4)$, 10^{-10}

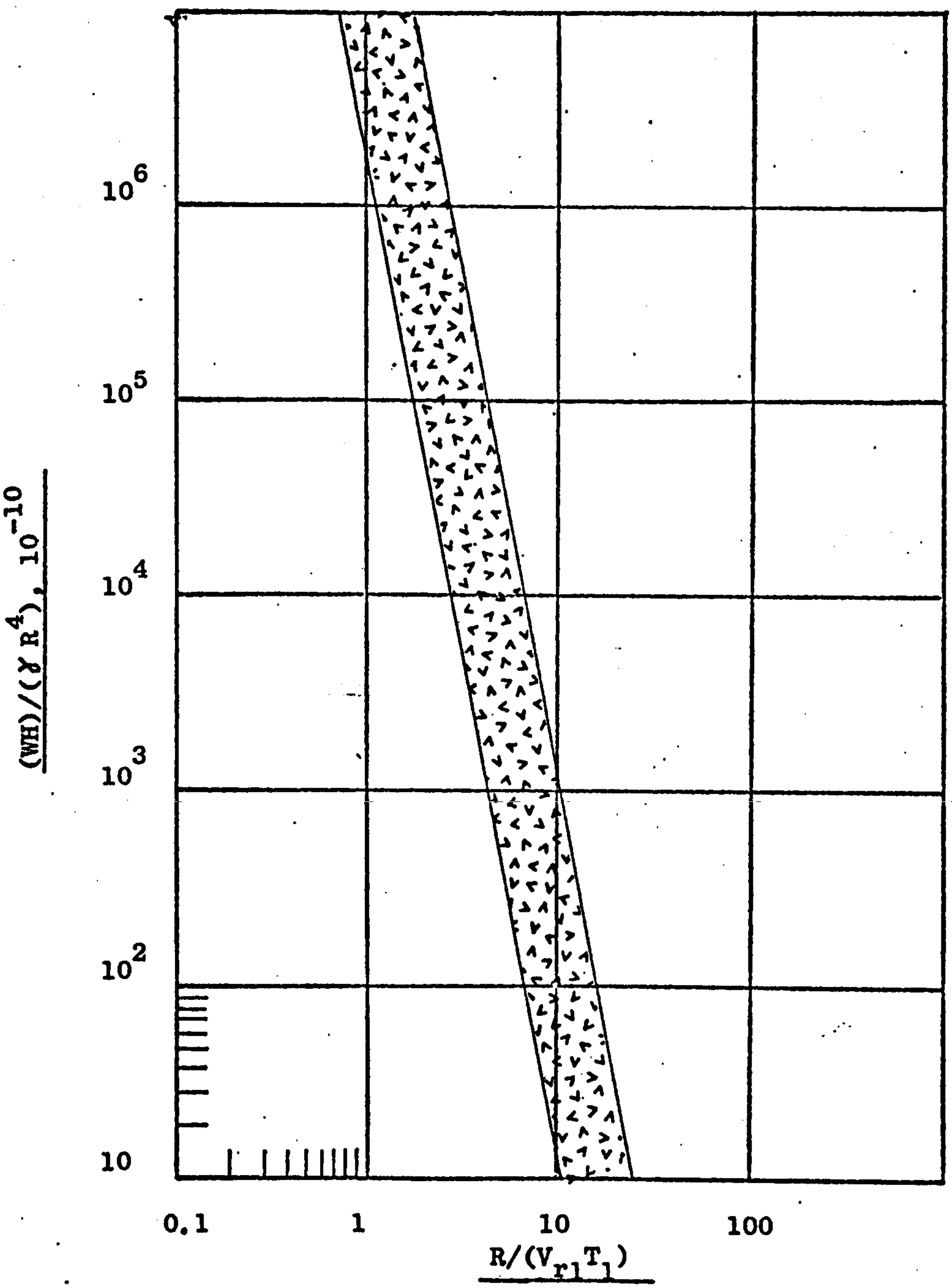

10^6
10^5
10^4
10^3
10^2
10
(WH)/(γ R^4), 10^-10
0.1
1
10
100
R/(V_r1 T_1)

Unclassified

Security Classification

DOCUMENT CONTROL DATA - R & D

(Security classification of title, body of abstract and indexing annotation must be entered when the overall report is classified)

1. ORIGINATING ACTIVITY (Corporate author) U. S. Army Engineer Waterways Experiment Station Vicksburg, Mississippi	2a. REPORT SECURITY CLASSIFICATION Unclassified 2b. GROUP

3. REPORT TITLE

FUNDAMENTAL EXPERIMENTS IN GROUND SHOCK PHENOMENOLOGY

4. DESCRIPTIVE NOTES (Type of report and inclusive dates)

Final report

5. AUTHOR(S) (First name, middle initial, last name)

James G. Wallace
Jack Fowler

6. REPORT DATE	7a. TOTAL NO. OF PAGES	7b. NO. OF REFS
March 1973	65	3

8a. CONTRACT OR GRANT NO. b. PROJECT NO. 4A0621101A91D c. d.	9a. ORIGINATOR'S REPORT NUMBER(S) Miscellaneous Paper N-73-2 9b. OTHER REPORT NO(S) (Any other numbers that may be assigned this report)

10. DISTRIBUTION STATEMENT

Approved for public release; distribution unlimited.

11. SUPPLEMENTARY NOTES	12. SPONSORING MILITARY ACTIVITY Office, Chief of Engineers, U. S. Army Washington, D. C.

13. ABSTRACT

This paper describes a technique which can be used to create a well-defined directly induced seismic energy source exclusive of any airblast effects. It was shown that spherical masses impacting on the ground surface produced ground motions which could be correlated with motions produced by high explosion tests. The tests conducted during this study included 26 spheres of varying size and density with weights ranging from 9 lb to 2,275 lb. Geophones were placed at various distances from the impact epicenter to measure ground surface particle velocity. An accelerometer was mounted on the sphere to monitor the deceleration during impact on the ground surface. Empirical equations were developed for the peak vertical particle velocity, period, wave group velocity and impact crater dimensions in terms of energy level and distance from the epicenter of the source. The impact data obtained at WES were correlated with high explosive data obtained during the MIXED COMPANY test conducted in Colorado.

DD FORM 1 NOV 65 1473 REPLACES DD FORM 1473, 1 JAN 64, WHICH IS OBSOLETE FOR ARMY USE.

Unclassified

Security Classification

Unclassified
Security Classification

14. KEY WORDS	LINK A		LINK B		LINK C	
	ROLE	WT	ROLE	WT	ROLE	WT
Ground shock						
Seismic response						

Unclassified
Security Classification